Inorganic Chemistry

Article

pubs.acs.org/IC

Pyrazole and Pyrazolate as Ligands in the Synthesis and Stabilization of New Palladium(II) and (III) Compounds

Francisco Estevan,[†] Pipsa Hirva,*[,‡] Albert Ofori,[‡] Mercedes Sanaú,[†] Tanja Šepec,[†] and M[a]Angeles Úbeda*[,†]

[†]Departament de Química Inorgànica, Universitat de València, Dr. Moliner 50, 46100-Burjassot, València, Spain

[‡]Department of Chemistry, University of Eastern Finland, Joensuu Campus, P.O. Box 111, FI-80101 Joensuu, Finland

Supporting Information

ABSTRACT: The versatility of pyrazole/pyrazolate as ligands has allowed the synthesis and the structural characterization of four different types of new orthometalated palladium compounds, for which DFT calculations have been performed in order to investigate their relative stabilities. $[Pd_2\{\mu\text{-}(C_6H_4)PPh_2\}_2\{\mu\text{-}(R,R'_2pz)\}_2]$ (R = R′ = H, **2a**; R = Br, R′ = H, **2b**; R = CH_3, R′ = H, **2c**; R = H, R′ = CH_3, **2d**; R = Br, R′ = CH_3, **2e**) compounds with *exo*-bidentate pyrazolatos are the first paddlewheel dinuclear palladium(II) compounds with pyrazolato bridging ligands described and characterized in the literature. In the process of the synthesis of **2a**, a new tetranuclear intermediate compound, $[Pd_4\{\mu\text{-}(C_6H_4)PPh_2\}_4(\mu\text{-pz})_2(\mu{-}OH)_2]$ (**3a**), has been isolated and structurally characterized. Compounds of the general formula $[Pd_2\{\mu\text{-}(C_6H_4)\text{-}PPh_2\}_2Br_2(R,R'_2pzH)_2]$ (R = R′ = H, **4a**; R = Br; R′ = H, **4b**; R = CH_3; R′ = H, **4c**; R = H; R′ = CH_3, **4d**; R = Br; R′ = CH_3, **4e**) with pyrazoles as monodentate ligands have also been obtained, in which, according to the QTAIM analysis, additional Br···HN_{pz} weak interactions stabilize their structure. The tetranuclear Pd_2Ag_2 compounds, $[Pd_2\{\mu\text{-}(C_6H_4)PPh_2\}_2\{\mu\text{-}(R,R'_2pz\text{-}Ag\text{-}R,R'_2pz)\}_2]$ (R = R′ = H, **5a**; R = Br; R′ = H, **5b**; R = CH_3, R′ = H, **5c**), showed a distorted tetrahedron disposition of the metal atoms. The QTAIM analysis revealed an enhanced stability because of additional metal−metal interactions. New palladium(III) compounds, $[Pd_2\{\mu\text{-}(C_6H_4)PPh_2\}_2\{\mu\text{-}(R,R'_2pz)\}_2Cl_2]$ (R = R′ = H, **6a**; R = Br, R′ = H, **6b**) were also synthesized by oxidation of compounds **2** with $PhICl_2$. DFT calculations highlighted their greater stability compared to that of similar compounds with N,N-donor ligands, such as formamidinatos and triazenidos.

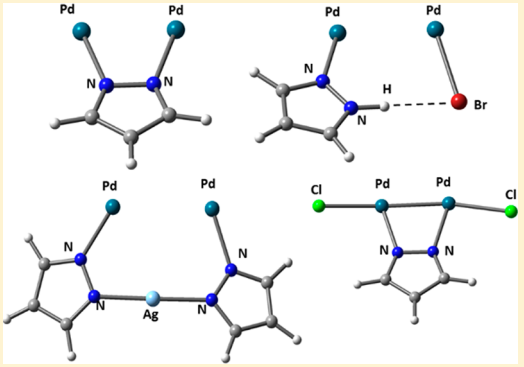

INTRODUCTION

Pyrazoles are well-known nitrogen donor ligands with versatile coordination chemistry, and they can act as neutral/anionic monodentate or also as *exo*/*endo*-bidentate anionic ligands.[1] As *exo*-bidentate ligands, the pyrazolatos can hold two metal atoms in close proximity with an appropriate metal−metal separation allowing a wide range of intermetallic separations (favorable distance of 2.4−4.6 Å).[1b,d,2] Therefore, they are suitable ligands to construct multimetal and metal−metal bond coordination systems.[1a−d,3]

The pyrazolato ligands form a variety of stable complexes with the platinum group metals. In the case of palladium in the oxidation state II, there are some structures of dinuclear homo-[4] and heteroleptic[2,5] pyrazolato palladium(II) compounds in which the dimetallic structure is only supported by two pyrazolato bridging ligands in an *exo*-bidentate fashion, giving an "open book" disposition for the square-planar environment of the palladium centers. Although the literature about these compounds is extensive, there are no structures of paddlewheel dinuclear palladium(II) complexes with pyrazolato bridging ligands.

In compounds with monocoordinated pyrazole ligands, the proton of the N−H bond can be replaced by metal ions such as Cu(I), Ag(I), and Au(I) giving heterometallic polynuclear complexes. In the literature, a few pyrazolate tetra- and hexaheterometallic compounds, $M_2M'_2$ (M = Pd, M′ = Cu,[4e,f] Ag,[4b−f,6a] Au[4e,6a]) and $M_2M'_4$ (M = Pd, M′ = Ag;[4f] M = Pt, M′ = Cu,[6b] Ag[4d,6b]) have been synthesized and some of them structurally characterized.

The chemistry of palladium in oxidation state III, despite the advances developed in the last ten years, continues to be poorly known.[7] Focusing on the chemistry of the dinuclear palladium(III) compounds with a Pd_2^{6+} core and M-M bond, a few of these have been well characterized since the first one was synthesized by Cotton and co-workers.[8] In the last few years, our research has focused on the chemistry of this type of palladium(III) compounds, with our group being the first who reported the synthesis of these complexes in high yield.[9] Moreover, Ritter and co-workers have characterized not only other discrete dinuclear[10] and chain-like[11] palladium(III)

Received: November 2, 2015

DOI: 10.1021/acs.inorgchem.5b02506
Inorg. Chem. XXXX, XXX, XXX−XXX

complexes with metal−metal bonds but also a transition state analogue for the oxidation of a palladium(II) compound to a palladium(III) one.[12]

Exploring the versatility of pyrazole/pyrazolato ligands, we present in this Article the synthesis, characterization, and the study of the stability of new orthometalated palladium compounds. Compounds of type **A** (Figure 1) are the first

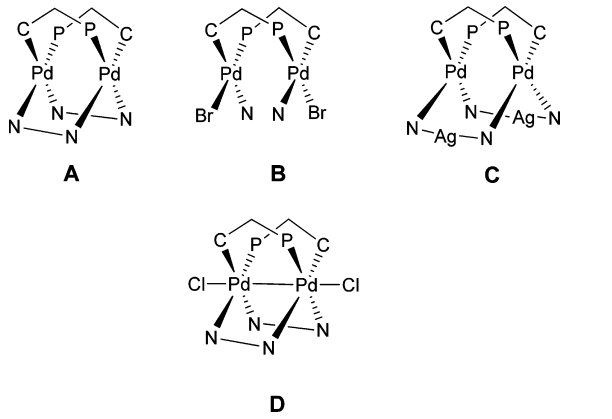

Figure 1. Dinuclear palladium(II) (**A**, **B**, and **C**) and palladium(III) (**D**) compounds.

paddlewheel dinuclear palladium(II) compounds with pyrazolato bridging ligands described and characterized in the literature. Compounds of type **B** (Figure 1) show the pyrazole acting as a neutral monodentate ligand. Tetranuclear Pd_2Ag_2 compounds were also synthesized and characterized, type **C** (Figure 1). The oxidation of compounds **A** with $PhICl_2$ allowed the synthesis of new palladium(III) compounds, type **D** (Figure 1), to which the pyrazolato ligands have provided high stability.

DFT calculations have been performed for all the different palladium(II) and palladium(III) pyrazolato complexes of types **A**−**D** to investigate their relative stabilities. The calculations focus on how the various pyrazolato derivatives assist in stabilizing the palladium compounds. Moreover, topological charge density analysis according to the Quantum Theory of Atoms in Molecules (QTAIM) was performed on the compounds to evaluate the nature of the intramolecular interactions.

RESULTS AND DISCUSSION

A. Pyrazolate Palladium(II) Compounds. *$[Pd_2\{\mu$-(C_6H_4)-$PPh_2\}_2\{\mu$-$(R,R'_2pz)\}_2]$ Compounds: Synthesis and Characterization.* Compounds **2** of general formula $[Pd_2\{\mu\text{-}(C_6H_4)\text{-}PPh_2\}_2\{\mu\text{-}(R,R'_2pz)\}_2]$ were obtained from the tetranuclear palladium(II) compound **1**, $[Pd_4(\mu\text{-}Br)_4\{\mu\text{-}(C_6H_4)PPh_2\}_4]$, following the procedures described in Scheme 1 **I**. (i) Compounds **2a** (R = R′ = H), **2b** (R = Br; R′ = H), and **2c** (R = CH_3; R′ = H) were obtained by the reaction of **1** with the corresponding potassium pyrazolate (ratio = 1:4), via a cationic dinuclear intermediate. (ii) Compounds **2d** (R = H; R′ = CH_3) and **2e** (R = Br; R′ = CH_3) were synthesized by direct reaction of **1** with the corresponding silver pyrazolate (ratio = 1:4).

The ^{31}P NMR spectra of compounds **2a**−**e** showed a single signal, and their δ (ppm) values are listed in Table 1. Comparing these δ values with those obtained for orthometalated compounds with N−N-donor ligands, formamidinatos or triazenidos, they are shifted toward lower fields.

Compounds **2b**−**e** were structurally characterized by single-crystal X-ray diffraction methods. Figures 2 and S1 show the perspective view for compounds **2b**−**e**. Selected bond distances and angles for the four compounds are given in Table 2.

The four compounds show similar paddlewheel structures in which the bimetallic unit is supported by two orthometalated phosphanes in a head-to-tail arrangement and two pyrazolato ligands completing the palladium square planar coordination mode.

These compounds with C_2 symmetry show a chirality that arises from the configurational arrangement of the molecule. Each crystal is racemic containing the mixture of *S* and *R* molecules based on the sign of the P−Pd···Pd−P torsion angles (Figure S2). The absolute values of these angles are between 89.36° to 93.87° (Table S1). Moreover, a second point of chirality in these molecules can be induced by the conformational arrangement of the ligands. P−Pd···Pd−C torsional angle senses were designated with the nomenclature *P* and *M*. The complete description of the stereochemistry in these molecules can require specification of the two senses of chirality *S* or *R* and *P* or *M* (Figure S3).[13]

Compound **2b** shows a stereochemistry of S_M/R_P with an absolute value for P−Pd···Pd−C torsion angle of 3.62° (Table S1). However, **2c**−**e** have a disposition practically eclipsed of the ligands (P−Pd···Pd−C torsion angles around 0) (Table S1). Similar paddlewheel carboxylato and triazenido derivatives also showed a stereochemistry of S_M/R_P.[9f,13]

The Pd−Pd distances from 2.6724(7) to 2.684(12) Å are shorter than the sum of the van der Waals palladium radii (3.26 Å). We have included in this Article a charge density analysis at the Pd−Pd bond critical points (BCPs), which supports a Pd(II)···Pd(II) interaction with some electron sharing (See section C and Table S2). Furthermore, this interaction can be seen in the experimental UV−vis spectra, which have been interpreted via simulating the spectra by TD-DFT calculations (Figure S4). According to the computational results, the lowest energy bands mainly consist of transitions between the antibonding Pd(d) orbitals mixed with the p-orbitals of nitrogens of the pyrazolato ligands, which is an indication of Pd−Pd contacts. These bands are clearly visible in both the experimental UV−vis and the simulated spectra. The frontier molecular orbital analysis is also presented to show the different transitions involved (Figure S5).

Comparing the Pd−Pd distances observed in orthometalated dinuclear palladium(II) compounds with N,N-donor ligands, we observed that the pyrazolato derivatives show shorter distances than those of the formamidinato derivatives (2.711−2.717 Å),[9b] and in the case of the triazenido compounds without axial interaction, they are similar (2.6618−2.6794 Å).[9f] These compounds also showed Pd(II)···Pd(II) interactions that have been studied earlier.[9c−g]

The dimetallic pyrazolato palladium structures described in the literature are supported by only two pyrazolato bridging ligands in an *exo*-bidentate fashion and showed longer Pd−Pd distances in a typical range of 3.00 to 3.46 Å.[4,5] Some specific compounds have even higher values (3.645 Å).[4a]

The different Pd−N distances observed in each compound reflect the *trans* influence of the donor atoms from the orthometalated phosphane. With the exception of compound **2b**, the Pd(1)−N(1) distances (2.085−2.099 Å) with N *trans* to P are shorter than Pd(1)−N(2) ones where N is *trans* to C (2.137−2.147 Å) as expected. In compound **2b**, both distances Pd−N are similar, and no appreciable difference in *trans*

DOI: 10.1021/acs.inorgchem.5b02506
Inorg. Chem. XXXX, XXX, XXX−XXX

Scheme 1[a]

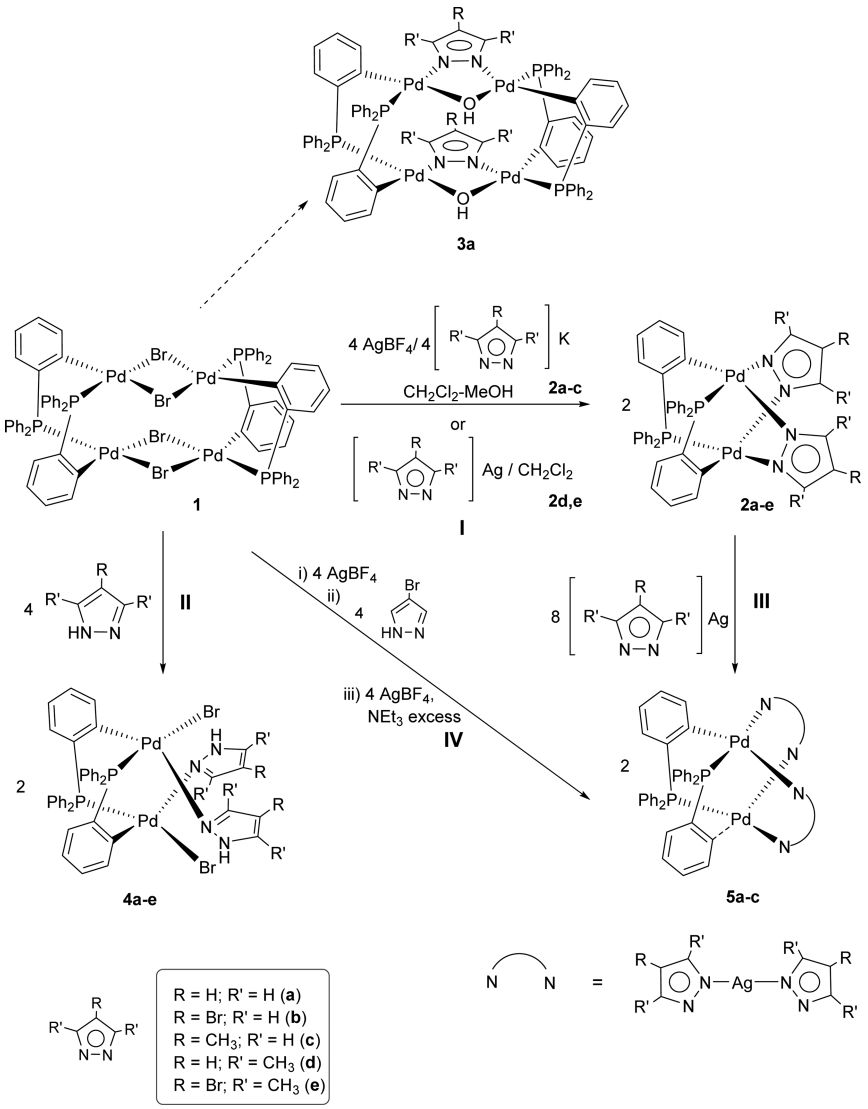

[a]**I**: synthesis of $[Pd_2\{\mu\text{-}(C_6H_4)PPh_2\}_2\{\mu\text{-}(R,R'_2pz)\}_2]$ compounds. **II**: synthesis of $[Pd_2\{\mu\text{-}(C_6H_4)PPh_2\}_2Br_2(R,R'_2pzH)_2]$ compounds. **III**: synthesis of $[Pd_2\{\mu\text{-}(C_6H_4)PPh_2\}_2\{\mu\text{-}(R,R'_2pz\text{-}Ag\text{-}R,R'_2pz)\}_2]$ compounds. **IV**: synthesis of **5b** by an alternative procedure.

Table 1. ^{31}P NMR Spectroscopy Data at 298 K for Palladium(II) Compounds

$[Pd_2\{\mu\text{-}(C_6H_4)PPh_2\}_2\{\mu\text{-}(R,R'_2pz)\}_2]$		$[Pd_2\{\mu\text{-}(C_6H_4)PPh_2\}_2Br_2(R,R'_2pzH)_2]$		$[Pd_2\{\mu\text{-}(C_6H_4)PPh_2\}_2\{\mu\text{-}(R,R'_2pz\text{-}Ag\text{-}R,R'_2pz)\}_2]$	
compound	δ (ppm)	compound	δ (ppm)	compound	δ (ppm)
2a	37.4	**4a**	18.7	**5a**	19.4
2b	37.7	**4b**	18.9	**5b**	19.1
2c	37.5	**4c**	18.7	**5c**	19.5
2d	34.4	**4d**	21.2		
2e	35.4	**4e**	20.7		

influence is observed. The N−Pd−N angles are comparable to the other palladium(II) compounds with two pyrazolato bridging ligands.[4,5]

Structural data for compound **2b−e** are included in the Supporting Information (Table S3, dihedral angle formed by the two Pd-N-N-Pd fragments; Table S4, dihedral angles between the coordination planes of the palladium atoms; and Table S5, bow angles between the planes defined by N1-N2-N1-N2 and N1-Pd-N2).

As the most relevant conformation features for dinuclear pyrazolate palladium compounds, Pérez and Espinosa collected the Pd−Pd distances and the relative positions of the bridging pyrazolato ligands: pyrazolate ring centroids distance (d_{pz^*}−d_{pz^*}) and the angle between the pyrazolate rings (β).[5d] Compounds **2b−e** with d_{pz^*}−d_{pz^*} between 4.243 and 4.479 Å and compounds **2b,d,e** with β from 95.39° to 92.47° (Table S6) show values within the observed range in other pyrazolate compounds.[4,5] **2c** has a β value of 110.55°, which is the highest observed in compounds **2b−e**.

According to QTAIM calculations, there are intermolecular interactions that occur between the pyrazolate rings and the solvent of crystallization (CH_2Cl_2) in **2c** (shown in Figure S6). Similar interactions were not obtained with other compounds **2b,d,e**, in which the solvent of crystallization is not located between the rings, and therefore, they have only very weak hydrogen bonding interactions between the terminal substituents and the orthometalated phosphanes of another

DOI: 10.1021/acs.inorgchem.5b02506
Inorg. Chem. XXXX, XXX, XXX−XXX

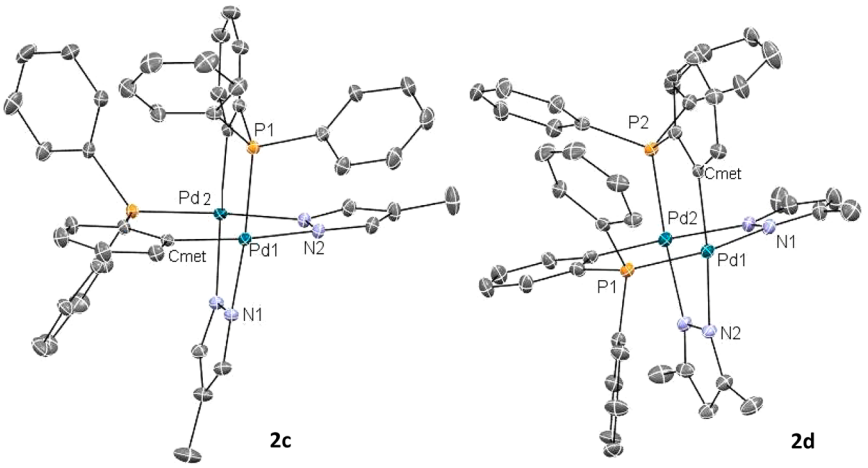

Figure 2. Perspective view of compounds **2c** and **2d** with the H atoms omitted for clarity. Ellipsoids are drawn at 25% probability.

Table 2. Selected Distances (Å) and Angles (Deg) for Compounds 2b–e

	2b	2c	2d	2e
Pd(1)-Pd(2)	2.6794(7)	2.6724(7)	2.684(12)	2.6800(9)
Pd(1)-P(1)	2.2702(13)	2.2438(12)	2.241(3)	2.2437(13)
Pd(1)- N(1)	2.139(4)	2.087(4)	2.085(11)	2.099(4)
Pd(1)- N(2)	2.127(4)	2.146(4)	2.137(10)	2.147(4)
Pd(1)-C(met)	1.990(5)	2.004(5)	2.0048(12)	2.004(5)
N(2)-Pd(1)-C(met)	168.11(18)	165.49(18)	165.3(4)	165.41(16)
N(1)-Pd(1)-N(2)	86.59(16)	88.01(15)	87.5(4)	87.07(16)

molecule. The somewhat larger β value of **2c** results from the solvent molecule situated in between the pyrazolate rings and can be attributed to the packing effects.

In spite of the multiple attempts, no suitable crystals of compound **2a** were obtained, so it has not been structurally characterized. In one of the processes of crystallization, few crystals of a new compound **3a** could be isolated (Scheme 1). The ^{31}P NMR spectrum of these crystals showed only one signal at 23.6 ppm, a value that is closer to that observed for the tetranuclear compound **1**: 26.7 ppm than for the dinuclear **2a**, 37.4 ppm. All the attempts to synthesize this compound, **3a**, have been unsuccessful. Luckily, compound **3a** was structurally characterized by single-crystal X-ray diffraction methods. Figure 3 shows its perspective view and also includes selected bond distances and angles.

The molecular structure of **3a** consists of a distorted parallelogram of four palladium atoms with alternate sides bridged either by two orthometalated phosphanes in a head-to-tail arrangement or by two different ligands, hydroxo and pyrazolato. Each palladium has a slightly distorted square planar coordination, bound to one C, one P, one N, and one O that bridge two palladium atoms. The hydroxo bridges are not symmetric since the Pd–O distances are larger when O is *trans* to C than when it is *trans* to P, highlighting a higher *trans* influence of the carbon atom (2.102 and 2.078 Å vs 2.051 Å). This influence is also reflected in the Pd–N distances (2.145 and 2.140 Å vs 2.079 and 2.074 Å). The distances between the palladium atoms across the orthometalated ligands are considerably closer than across the hydroxo and pyrazolato ligands (3.120 and 3.113 Å vs 3.581 and 3.563 Å). According to the computational analysis, the increase in the bond distances leads to reduction in the strength of the Pd···Pd interactions since the interaction energy is −19.5 kJmol^{-1} at the shortest Pd–Pd interaction in **3a** compared to approximately −67 kJmol^{-1} in compounds **2a**. However, the HOMO–LUMO gap in **3a** was found comparable with that of compounds **2a** (e.g., 3.85 and 3.86 eV in compounds **3a** and **2a**, respectively), indicating similar stability for the compounds.

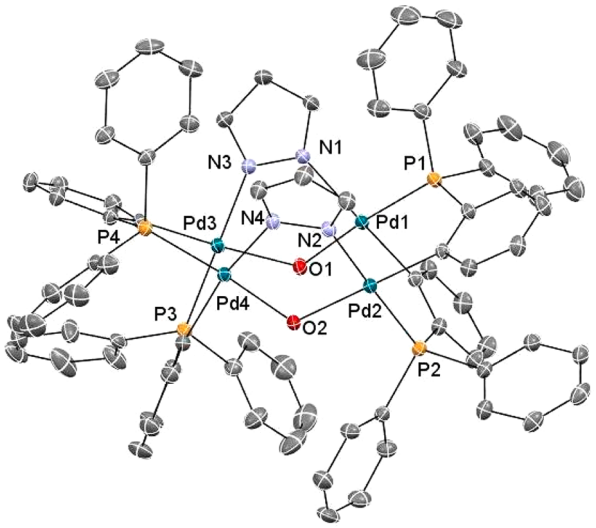

Figure 3. Perspective view of compound $[Pd_4\{\mu\text{-}(C_6H_4)PPh_2\}_4(\mu\text{-}pz)_2(\mu\text{-}OH)_2]$, **3a**, with the H atoms omitted for clarity. Ellipsoids are drawn at 25% probability. Selected bond distances (Å) and angles (deg) are Pd1–Pd2, 3.1135(4); Pd3–Pd4, 3.1200(4); Pd1–O1, 2.051(3); Pd2–O2, 2.078(3); Pd1–P1, 2.2364(11); Pd1–N1, 2.145(4); P1–Pd1–O1, 174.85(8); N1–Pd1–Cmet, 160.40(14).

We considered that the small excess of KOH used in the pyrazole deprotonation provided the hidroxo groups for the serendipitous formation of **3a** serendipitous.

DOI: 10.1021/acs.inorgchem.5b02506
Inorg. Chem. XXXX, XXX, XXX–XXX

In the literature, there are structures of palladium(II) complexes with μ-hydroxo groups that contain Pd(μ-OH)$_2$Pd,[14] Pd(μ-OH)Pd,[15] or mixed Pd(μ-OH)(μ-L)Pd[16] cores. The Pd−Pd distance of 3.581 and 3.563 Å in the Pd(μ-OH)(μ-pz)Pd core is the greatest observed among the compounds with mixed bridging ligands, in which one of them is a hydroxo group. Only one tetranuclear palladium compound is described in the literature, and it contains two Pd(μ-OH)(μ-O$_2$CMe)Pd cores bridged by two metalated bis(2-pyridyloxy) naphthalene ligands with Pd−Pd distances of 3.052 and 3.034 Å.[16k]

Comparing compound **3a** with the tetranuclear starting product, [Pd$_4$(μ-Br)$_4$\{μ-(C$_6$H$_4$)PPh$_2$\}$_4$] (**1**), it can be observed that **1** shows shorter Pd−Pd distances between the palladium atoms across the orthometalated ligands (3.07 vs 3.120 and 3.113 Å) and longer distances across Pd(μ-Br)$_2$Pd cores than across Pd(μ−OH)(μ-pz)Pd ones (3.64 vs 3.581 and 3.563 Å).

[Pd$_2$\{μ-(C$_6$H$_4$)PPh$_2$\}$_2$Br$_2$(R,R′$_2$pzH)$_2$] Compounds: Synthesis and Characterization. The reaction of **1** with the corresponding pyrazole in a 1:4 ratio resulted in the synthesis of [Pd$_2$\{μ-(C$_6$H$_4$)PPh$_2$\}$_2$Br$_2$(R,R′$_2$pzH)$_2$] compounds (R = R′ = H, **4a**; R = Br; R′ = H, **4b**; R = CH$_3$; R′ = H, **4c**; R = H; R′ = CH$_3$, **4d**; R = Br; R′ = CH$_3$, **4e**) (Scheme 1 **II**). The ^{31}P NMR spectra of compounds **4a−e** showed a single signal, and their δ (ppm) values are listed in Table 1.

Compounds **4a,c,d** were structurally characterized by single-crystal X-ray diffraction methods. Figures 4 and S7 show the perspective view for these compounds. Selected bond distances and angles for the three compounds are given in Table 3.

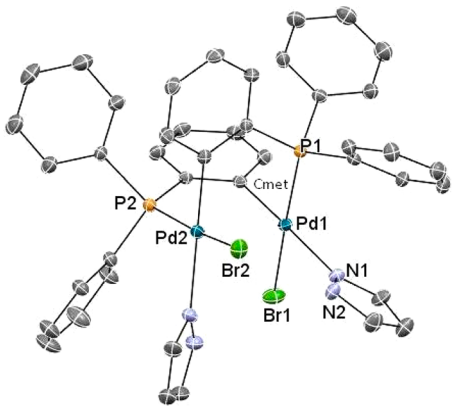

Figure 4. Perspective view of compound **4a** with the H atoms omitted for clarity. Ellipsoids are drawn at 25% probability.

In these compounds, the bimetallic unit is only supported by two orthometalated phosphanes in a head-to-tail arrangement, the palladium square planar coordination mode is completed by one bromido and the corresponding pyrazole as monocoordinated ligands. In compounds **4a,c,d**, the Br atom occupies the position *trans* to P. The similarity of chemical shifts in the ^{31}P NMR spectra leads us to think that this structure is maintained in compounds **4b,e**.

Compounds **4** are also chiral (symmetry C$_2$). In the case of compound **4a**, its asymmetric unit contains one molecule of each enantiomer. The stereochemistry (Figure S8) and P-Pd···· Pd-P/C-Pd···Pd-P torsion angles (Table S7) are included in the Supporting Information. The presence of only two bridging ligands supporting the dinuclear units in **4a,c,d** gives less rigidity to the structures, and consequently, the C-Pd ···· Pd-P torsion angles are larger than those in compounds **2b−e**. **4a** and **4c** have the stereochemistry S_M/R_P, while **4d** shows a S_P/R_M one. In these compounds, the Pd−Pd distances around 3 Å are larger than those observed in compounds **2b−e** (~2.68 Å).

According to the QTAIM analysis, weak Br···HN$_{pz}$ interactions were observed for compounds **4**. These intramolecular interactions for compound **4a** are shown in Figure S9. The delocalization index (Ω(Br, H)) and the interaction energy of 0.123 and −24 kJmol^{-1}, respectively, indicate stabilizing intramolecular hydrogen bonding interactions between Br and H−N$_{pz}$, which can be suggested to affect the geometry of the molecule and also the electronic properties such as NMR spectra. In this aspect, it is found in the ^{1}H NMR spectra of compounds **4** that the signal corresponding to NH changes from a broad signal in pyrazoles to a sharp signal at similar chemical shift values.

[Pd$_2$\{μ-(C$_6$H$_4$)PPh$_2$\}$_2$\{μ-(R,R′$_2$pz-Ag-R,R′$_2$pz)\}$_2$] Compounds: Synthesis and Characterization. The reaction of **1** with a slight excess of Ag(R,R′$_2$pz) (R = R′ = H; R = Br, R′ = H; R = CH$_3$, R′ = H) highlighted in each case the formation of a new compound in addition to the corresponding compound **2**. These new heterometallic tetranuclear complexes, [Pd$_2$\{μ-(C$_6$H$_4$)PPh$_2$\}$_2$\{μ-(R,R′$_2$pz-Ag-R,R′$_2$pz)\}$_2$] (R = R′ = H, **5a**; R = Br; R′ = H, **5b**; R = CH$_3$, R′ = H, **5c**) were obtained as the only products when the corresponding silver pyrazolate reacted with **1** at a ratio of 8.5:1 (Scheme 1, **III**).

When **1** reacted with silver salts of bulky pyrazolates (R = H ; R′ = CH$_3$; R = Br; R′ = CH$_3$), no formation of **5d,e** was observed, and **2d,e** were the only products of the synthesis.

Compound **5b** was also obtained following an alternative procedure involving the deprotonation with NEt$_3$ of the 4-bromo-1*H*-pyrazole coordinated in the intermediate compound [Pd$_2$\{μ-(C$_6$H$_4$)PPh$_2$\}$_2$(R,R′$_2$pz)$_4$](BF$_4$)$_2$ (R = Br, R′ = H) and subsequent reaction with AgBF$_4$ (Scheme 1 **IV**).

The ^{31}P NMR data for compounds **5a−c** are listed in Table 1. In each case, the signal appears shifted toward high fields (~19 ppm), compared with those observed for **2a−c** (~37 ppm). The ^{1}H NMR and ^{13}C NMR spectra of **5a−c** show the nonequivalence of the coordinated pyrazolate groups. One of

Table 3. Selected Distances (Å) and Angles (Deg) for Compounds 4a,c,d

	4a (*R*)	4a (*S*)	4c	4d
Pd(1)-Pd(2)	3.0732(12)	3.1387(14)	3.0846(7)	3.1758(5)
Pd(1)-P(1)	2.2634(16)	2.2667(18)	2.2710(13)	2.2580(9)
Pd(1)- N(1)	2.131(5)	2.138(6)	2.145(4)	2.123(3)
Pd(1)- Br(1)	2.4934(11)	2.4961(19)	2.5162(7)	2.5118(5)
Pd(1)-C(met)	1.992(6)	1.994(6)	1.997(5)	2.001(3)
N(1)-Pd(1)-C(met)	172.8(2)	173.3(2)	175.14(18)	168.04(14)
Br(1)-Pd(1)-C(met)	86.28(16)	86.13(17)	85.94(14)	88.62(10)

DOI: 10.1021/acs.inorgchem.5b02506
Inorg. Chem. XXXX, XXX, XXX−XXX

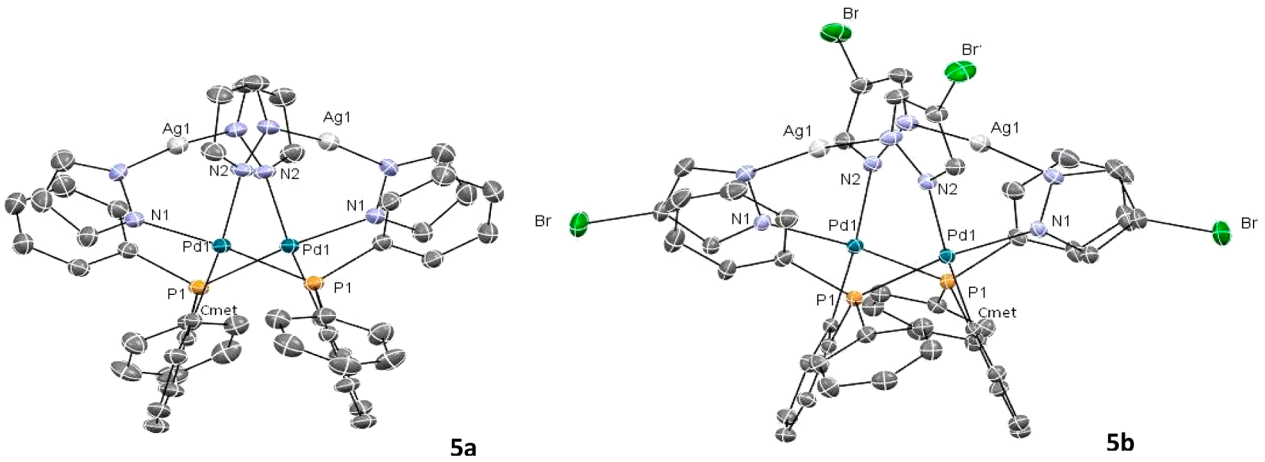

Figure 5. Perspective view of compounds **5a** and **5b** with the H atoms omitted for clarity. Ellipsoids are drawn at 25% probability.

the pyrazole rings is bonded to Pd in *trans* position to P, while the other is in *trans* position to C.

Compounds **5a,b** were structurally characterized by single-crystal X-ray diffraction methods. Figure 5 shows their perspective views. Selected bond distances and angles for both compounds are given in Table 4.

Table 4. Selected Distances (Å) and Angles (Deg) for Compounds 5a and 5b

	5a	5b
Pd(1)-N(1)	2.056(6)	2.072(4)
Pd(1)-N(2)	2.118(6)	2.122(4)
Pd(1)-C(met)	2.052(7)	2.032(4)
N(1)-Pd(1)-P(1)	172.0(3)	166.51(11)
N(1)-Pd(1)-C(met)	90.4(3)	89.31(16)

Compounds **5a,b** are tetranuclear complexes containing two palladium and two silver atoms. Both palladium atoms are supported by two orthometalated phosphanes in a head-to-tail arrangement and two anionic R,R′$_2$pz-Ag-R,R′$_2$pz groups acting as bridging ligands. Both metal centers show their usual coordination mode, square planar for Pd(II) and linear for Ag(I), with the N−Ag−N angles of 171.8(3)° for **5a** and 170.07(16)° for **5b**.

The steric requirements of the R,R′$_2$pz-Ag-R,R′$_2$pz (N−Ag−N distances of 4.181 (**5a**) and 4.2013 Å (**5b**)) versus R,R′$_2$pz, inflate the whole molecules **5a,b**. The Pd−Pd distances are 3.573 and 3.388 Å, respectively, while this distance is only 2.6794(7) Å for **2b**. Other significant changes correspond to the P−Pd···Pd−C and N−Pd···Pd−N torsion angles (Tables S1 and S7). Other structural data are given in Table S4. Compounds **5a,b** are also chiral and show a stereochemistry of S_M/R_P. (Figure S10 and Table S7).

The Pd−N bond lengths reflect the *trans* influence of the donor atoms from the orthometalated phosphane. These values as well as the Ag−N ones are in the range found in other related compounds.[4−6] The Ag atoms are located 3.427 (**5a**) and 3.566 (**5b**) Å from each other. The Ag···Ag distances in [Ag(pz)]$_3$ are 3.414, 3.414, and 3.449 Å.[17] The N−Ag−N and N−Ag−N vectors are not parallel, with torsion angles of 32.96° (**5a**) and 36.09° (**5b**).

It can be considered, that each molecule contains a metal tetrahedron of Pd_2Ag_2 formulation (Figure 6) in which the Pd···Pd edge is supported by two orthometalated phosphanes,

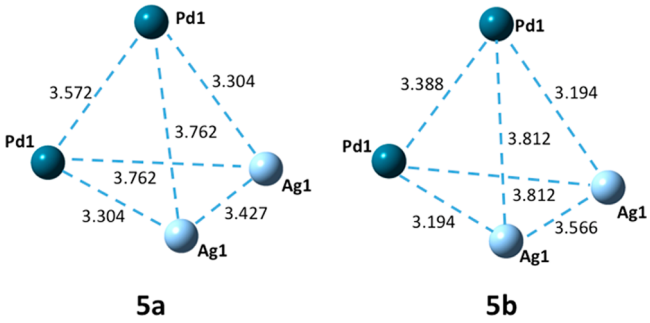

Figure 6. Metal tetrahedron of Pd_2Ag_2 in compounds **5a,b**.

the four Pd···Ag edges by a pyrazolate ligand each, and the Ag···Ag edge is not supported by any ligand. Two silver atoms are close to each palladium with different Pd···Ag distances.

There are different metal−metal interactions, which were observed in complexes **5**. The Pd···Pd, Pd···Ag, and Ag···Ag interactions were found in the QTAIM analysis and are fully discussed in the computational section C.

All of the tetranuclear Pd_2Ag_2 compounds structurally characterized in the literature show a distorted tetrahedron disposition of the metal atoms.[4b−f,6a] The intermetallic distances are summarized in Table 5.

B. Pyrazolate Palladium(III) Compounds. In order to obtain dinuclear palladium(III) compounds of the formula [Pd$_2${μ-(C$_6$H$_4$)PPh$_2$}$_2${μ-(R,R′$_2$pz)}$_2$Cl$_2$], compounds **2a−e** were oxidized with PhICl$_2$ at 223 K. Only compounds with R = R′ = H (**6a**) and R = Br, R′ = H (**6b**) (Scheme 2) were stable enough to be synthesized and characterized.

The ^{31}P NMR spectrum showed in both compounds only a single signal that appears shifted toward high fields by around 20 ppm relative to the observed signals for **2a** and **2b**. In agreement with the literature, this fact indicates the formation of palladium(III) compounds.[9]

In comparison with other palladium(III) compounds previously synthesized by our group, compounds **6a** and **6b** were particularly stable at room temperature. Despite their relative stability, both compounds have been synthesized and characterized by ^{13}C, ^{1}H, and ^{31}P NMR spectroscopy at low temperature (223 K). The ^{31}P NMR spectra of these compounds showed a single signal at δ values of 17.3 (**6a**) and 18.2 (**6b**) ppm.

DOI: 10.1021/acs.inorgchem.5b02506
Inorg. Chem. XXXX, XXX, XXX−XXX

Table 5. Metal−Metal Distances (Å) for the tetranuclear Pd_2Ag_2 Compounds Structurally Characterized in the Literature

compound	ref	metal−metal distances (Å)					
		Pd1-Pd2	Pd1-Ag1	Pd1-Ag2	Pd2-Ag1	Pd2-Ag2	Ag1-Ag2
$Pd_2Ag_2(\mu\text{-}3\text{-}t\text{-Bupz})_6{\cdot}2CH_3CN$	4d	3.380	3.495	3.515	3.264	3.341	4.5919
$Pd_2Ag_2(\mu\text{-dmpz})_6$	4e	3.513	3.303	3.185	3.164	3.382	3.195
$Pd_2Ag_2(\mu\text{-dmpz})_4(\mu\text{-}O_2CC_6H_4OCH_3)_2(DMSO)$	4b	3.427	3.065	3.417	2.959	3.467	2.921
$Pd_2Ag_2(\mu\text{-pz})_6{\cdot}3CH_3CN$	6a	3.4341	3.461	3.471	3.446	3.471	4.525
$Pd_2Ag_2(\mu\text{-pz})_6$	6a	3.423	3.460	3.421	3.439	3.399	4.541
							2.995[a]

[a]Ag···Ag intermolecular.

Scheme 2. Synthesis of $[Pd_2\{\mu\text{-}(C_6H_4)PPh_2\}_2\{\mu\text{-}(R,R'_2pz)\}_2Cl_2]$[a]

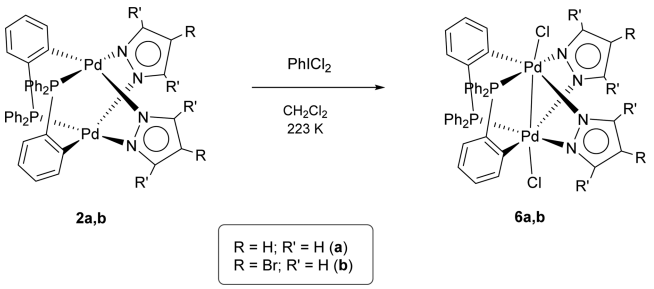

[a]R = R′ = H, **6a**; R = Br, R′ = H, **6b**.

Table 6. Selected Distances (Å) and Angles (Deg) for Compounds 6a and 6b

	6a	6b
Pd(1)-Pd(2)	2.5053(9)	2.5071(7)
Pd(1)-P(1)	2.272(2)	2.2837(14)
Pd(1)-N(1)	2.126(7)	2.127(4)
Pd(1)-Cl(1)	2.4159(19)	2.4162(14)
Pd(1)-C(met)	2.037(7)	2.040(5)
N(1)-Pd(1)-C(met)	90.68(3)	91.02(18)
Cl(1)-Pd(1)-C(met)	98.6(2)	98.80(14)
Cl(1)-Pd(1)-Pd(2)	163.83(6)	162.36(4)
N(1)-Pd(1)P(1)	89.61(19)	90.08(12)

Compounds **6a,b** were also structurally characterized by single crystal X-ray diffractions methods. The perspective views are shown in Figure 7, and selected bond distances and angles are given in Table 6.

The Pd_2^{6+} unit is bridged by two cisoid orthometalated phosphane ligands and two pyrazolatos in a head-to-tail arrangement. Two chloridos are coordinated in axial positions. The Pd−Pd distances of 2.505 and 2.507 Å in **6a** and **6b**, respectively, are the shortest among all of the characterized paddlewheel orthometalated palladium(III) derivatives and all of the dinuclear palladium(III) compounds described in the literature.[9,10]

Again, the different Pd−N distances observed in each compound reflect the *trans* influence of the donor atoms from the orthometalated phosphine. The dihedral angle formed by the two Pd-N-N-Pd fragments has values of 88.04° (**6a**) and 85.92° (**6b**) that are close to the observed in the dinuclear palladium(II) compounds **2** (Table S3). For both compounds, the axial chlorides are directed between the pyrazolato rings, and the Pd−Pd−Cl angle is 163.4° in **6a** and 162.3° in **6b**.

Compounds **6a,b** are also chiral. The stereochemistry (Figure S10) and P−Pd···Pd−P/C-Pd···Pd−P torsion angles (Table S7) are included in the Supporting Information. Some relevant conformation features relative to compounds **6a,b** are in Table S6.

C. DFT Studies of Pd (II) and (III) Compounds. The various compounds were optimized using the DFT level of theory and further analyzed by the QTAIM method to obtain information on their electronic stability. The properties of the electron density at the Pd−Pd bond critical point are shown in Table 7 for selected Pd(II) and Pd(III) pyrazolato compounds,

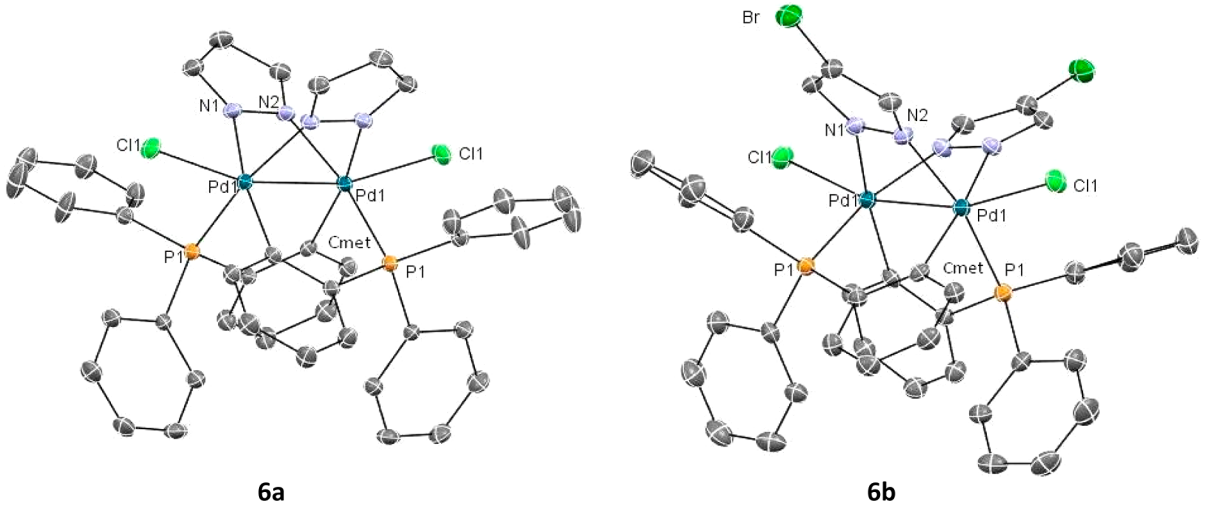

Figure 7. Perspective views of compounds **6a** and **6b** with the H atoms omitted for clarity. Ellipsoids are drawn at 25% probability.

DOI: 10.1021/acs.inorgchem.5b02506
Inorg. Chem. XXXX, XXX, XXX−XXX

Table 7. Properties of the Electron Density at the Pd−Pd BCPs According to the QTAIM Analysis of the Selected Palladium(II) and Palladium(III) Pyrazolato Compounds[a]

compounds	d(Pd−Pd) (Å)	ρ (eÅ^{-3})	$\lvert V\rvert/G$	Ω(Pd, Pd)	E_{INT} (kJmol^{-1})	HOMO−LUMO gap (eV)
2a	2.696	0.309	1.23	0.32	− 67.4	3.86
4a	3.031	0.162	1.17	0.23	− 25.1	4.08
6a	2.539	0.457	1.44	0.64	− 81.7	2.97
formamidinato[b]	2.761	0.288	1.23	0.33	− 60.1	3.53
triazenido[c]	2.692	0.311	1.23	0.35	− 67.4	3.49

[a]The properties are d(Pd−Pd) = optimized bond distance; ρ = local electron density at the BCP; $\lvert V\rvert/G$ = ratio of potential energy density and kinetic energy density; E_{INT} = interaction energy between two interacting atoms = $1/2{\cdot}V$(BCP); Ω(Pd, Pd) = delocalization index between Pd−Pd atoms and the HOMO-LUMO gap, in comparison to the previously studied N,N ligands. [b]$[Pd_2\{\mu\text{-}(C_6H_4)PPh_2\}_2\{\mu\text{-}(C_6H_5N\text{-}C\text{-}NC_6H_5)\}_2]$, ref 9c. [c]$[Pd_2\{\mu(C_6H_4)PPh_2\}_2\{\mu\text{-}(C_6H_5N\text{-}N\text{-}NC_6H_5)\}]_2$ ref 9f.

compared to those obtained for other complexes with N,N ligands. The complete analysis for all complexes studied here is presented in the Supporting Information (Table S2).

Notably, there is clear evidence that compounds **6** are relatively stable compared to other palladium(III) compounds with N,N ligands. Previously, the oxidation stability was studied by calculating the reaction energy of including two chlorido ligands into the axial position of the Pd(II) compounds according to the model reaction $[Pd_2\{\mu\text{-}(C_6H_4)PPh_2\}_2(\mu\text{-L})_2] + Cl_2 \rightarrow [Pd_2\{\mu\text{-}(C_6H_4)PPh_2\}_2(\mu\text{-L})_2Cl_2]$, resulting in reaction energies of −84 kJmol^{-1} and −88 kJmol^{-1} for the formamidinato $[Pd_2\{\mu\text{-}(C_6H_4)PPh_2\}_2\{\mu\text{-}(C_6H_5N\text{-}C\text{-}NC_6H_5)\}_2]$ and the triazenido $[Pd_2\{\mu\text{-}(C_6H_4)PPh_2\}_2\{\mu\text{-}(C_6H_5N\text{-}N\text{-}NC_6H_5)\}_2]$, respectively.[9f] The results of our present calculations show that compound **6b** has a larger reaction energy (ΔE_{react} = −197 kJmol^{-1}) than **6a** (ΔE_{react} = −182 kJmol^{-1}), both of which are substantially larger than the values in the formamidinatos and triazenidos. The difference can be explained by the larger steric requirements of the N−C−N and N−N−N ligands since both have bulky phenyl substituents, which can block the axial sites from the chlorido ligands, contrary to the pyrazolatos.

Further information on the relative stability can be obtained from the nature of the Pd−Pd interactions. The interaction energies for both **6a** and **6b** are very similar, −82 kJmol^{-1} at the Pd−Pd BCP, which are slightly larger than the ones obtained for Pd(III) complexes with formamidinato and triazenido ligands, −69 and −77 kJmol^{-1}, respectively. The larger interaction energy compared to that of **2a** is an indication of stronger Pd−Pd interaction in the Pd(III) compounds than the corresponding Pd(II), and according to the ratio of potential energy density and kinetic energy density, $\lvert V\rvert/G \gg 1$, the interaction approaches covalent bonding in the Pd(III) compounds. The same trend has been obtained previously for other Pd(II) and Pd(III) compounds.

The smaller interaction energy and also smaller electron density at the Pd−Pd BCP in compounds **4** can be attributed to the different bonding modes of the pyrazolato ligands. The monocoordinated bonding as well as the relatively large bromido ligands in the neighboring Pd forces longer Pd−Pd distances and therefore reduces the covalence and the strength of the interaction. However, the larger HOMO−LUMO gap in **4** indicated very stable compounds. This can be explained by the additional intramolecular Br···H−N_{pz} interactions in these compounds, which further stabilize the structure, as already discussed. The analysis of the hydrogen bonding interaction is presented in Figure S9.

The relative stability of compounds **5** was considered a special case and was well established by the DFT calculations and the QTAIM analysis. Geometrically, there were no significant differences observed between the optimized structures and the experimental structures. For example, the overall tetrahedron of the metal atoms was maintained (Figure 8).

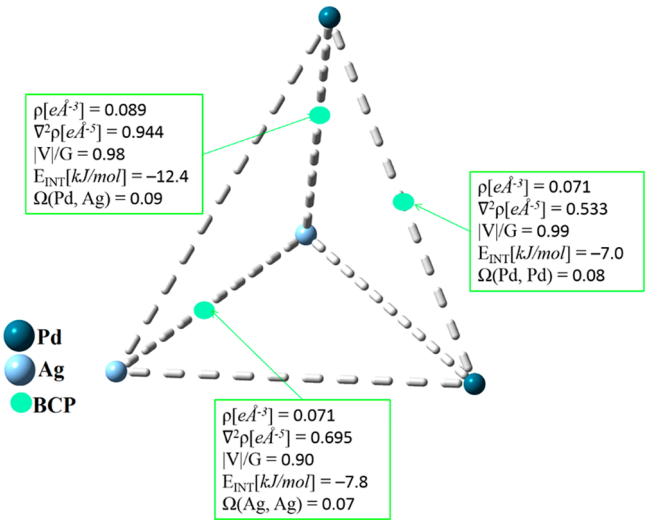

Figure 8. Properties of the electron density according to the QTAIM analysis of the optimized structure of **5a**. ρ[eÅ^{-3}] = electron density; $\nabla^2\rho$[eÅ^{-5}] = second derivative of ρ; $\lvert V\rvert/G$ = ratio between potential energy density and kinetic energy density; E_{INT}[kJ/mol] = interaction energy between two interacting atoms; Ω(M,M′) = delocalization index between M and M′ (where M = Pd or Ag and M′ = Pd or Ag). The phosphane and pyrazolato ligands were omitted for clarity, and only the metal core is shown.

The results in Table S2 show that compounds **5a−c** have the highest HOMO−LUMO gap of 4.5−4.7 eV compared with all of the other types of pyrazolato compounds. The enhanced stability is a result of additional metal−metal interactions in compounds **5**, as can be observed in Figure 8 along with the most important properties of the electron density at the corresponding BCPs. The small delocalization index of the metals, Ω(M, M′), and the small values of electron density (ρ) reveal that a limited amount of electron density is shared between metal atoms and that therefore, long bond distances result from the interactions. The different metal−metal interactions are very weak, with slight preference for the Pd···Ag interaction. For instance, at the Pd···Pd, Pd···Ag, and Ag···Ag BCPs the observed interaction energies were −7.0, −12.4, and −7.8 kJmol^{-1}, respectively, for complex **5a**. Even though the metal−metal interactions are very weak and mostly

DOI: 10.1021/acs.inorgchem.5b02506
Inorg. Chem. XXXX, XXX, XXX−XXX

noncovalent, they have an important role in stabilizing the molecular structure. It should also be noted that all complexes **5a−e** could be computationally optimized with rather similar characteristics of the metal−metal interactions (see Table S2), even if only **5a−c** could be experimentally obtained, and repeated attempts to prepare **5d,e** have been unsuccessful.

We also studied the favorability of forming compounds **5a−e** via the reaction of **2a−e** with silver pyrazolate salts AgL (Scheme 1, **III**). Table 8 lists the relative reaction energies of the reaction $[Pd_2\{\mu\text{-}(C_6H_4)PPh_2\}_2(\mu\text{-}L)_2]$+ 2 AgL → $[Pd_2\{\mu\text{-}(C_6H_4)PPh_2\}_2\{\mu\text{-}(LAgL)\}_2]$.

Table 8. Relative Reaction Energies [kJmol^{-1}] for the Formation of 5a−e from 2a−e and AgL[a]

reaction	ΔE [kJ mol^{-1}]
2a + 2 AgL → **5a**	0
2b + 2 AgL → **5b**	2
2c + 2 AgL → **5c**	2
2d + 2 AgL → **5d**	39
2e + 2 AgL → **5e**	36

[a]The energies are referenced to the first reaction.

Reaction of **2a** proved to be energetically the most favorable, and **2b** and **2c** were found to react rather similarly (in fact, the synthesis of **2a−c** by reaction of **1** with the corresponding silver pyrazolate always gave mixtures of compounds **2** and **5**). However, there was a rather large reduction in the stability of the products **5d** and **5e**, which had bulky R and R′ groups as substituents in the ligands. The smaller stability of **5d−e** could also been observed in their HOMO−LUMO gap, which was considerably reduced compared to that of the most stable product **5a** (4.62 and 4.26 eV for **5a** and **5e**, respectively). The stabilization of **2d,e** versus **5d,e** justifies that the latter compounds could not be synthesized.

CONCLUSIONS

New palladium(II) and (III) compounds have been synthesized and structurally characterized, which highlight the versatility and ability of stabilizing of the pyrazole and pyrazolate as ligands.

Compounds **2** are the first paddlewheel dinuclear palladium(II) compounds with pyrazolato bridging ligands described and characterized in the literature. A charge density analysis at the Pd−Pd BCPs supports a Pd(II)···Pd(II) interaction with some electron sharing. Compounds **4** with monocoordinated pyrazoles and bromide ligands show longer Pd−Pd distance, which involves a decrease of the covalency and the strength of this interaction. However, the relatively large HOMO−LUMO gap in **4a−e** indicates a high stability for these compounds that can be explained by the additional intramolecular Br···H−N_{pz} interactions able to stabilize their structure.

Heterotetranuclear compounds, **5a−c**, that contain a metal tetrahedron of Pd_2Ag_2 formulation have also been synthesized and structurally characterized. The relative stability of compounds **5a−c** can be considered a special case; they show the highest HOMO−LUMO gap of 4.5−4.7 eV compared with that of all the other types of pyrazolato compounds described in this Article. This fact can be attributed to additional metal−metal interactions; even though they are very weak and mostly noncovalent, they have an important role in stabilizing the molecular structure. Nevertheless, compounds **5d,e** with bulky R and R′ groups in the pyrazolato ligand could not be synthesized due to the stabilization of the **2d,e** precursors.

The new dinuclear palladium(III) compounds, **6a,b**, synthesized and characterized show the shortest Pd−Pd distances (2.505 (**6a**) and 2.507 (**6b**) Å) among all of the characterized paddlewheel orthometalated palladium(III) derivatives and all of the dinuclear palladium(III) compounds described in the literature. DFT calculations clearly evidence that these compounds **6** are relatively stable compared to other palladium(III) compounds with N,N ligands (formamidinato and triazenidos).

EXPERIMENTAL SECTION

All of the reactions were carried out under a dry nitrogen atmosphere using Schlenk techniques. Solvents were purified according to standard procedures. Commercially available reagents were used as purchased. $[Pd_4(\mu\text{-}Br)_4\{\mu\text{-}(C_6H_4)PPh_2\}_4]$,[18] **1**, and iodobenzene dichloride ($PhICl_2$)[19] were synthesized according to literature procedures. Solvent mixtures are v/v mixtures. Column chromatography was performed on silica gel (35−70 mesh). The chemicals (reactants and products) from this work pose no special hazard if the normal laboratory safety precautions are respected.

NMR spectra were recorded on Bruker 400 and 500 AMX spectrometers as solutions in deuterated chloroform or dichloromethane at 298 K and low temperature. Chemical shifts are reported in ppm, using tetramethylsilane, $Si(CH_3)_4$ (^{1}H, ^{13}C), and 85% H_3PO_4 (^{31}P) as references. The coupling constants (J) are in hertz (Hz). Elemental analysis was provided by SCSIE of University of Valencia.

Suitable single crystals of **2b−e**, **4a,c,d**, and **5a,b** were obtained at room temperature by layering hexane over dichloromethane solutions of the corresponding compounds. Single crystals of **6a,b** were obtained at 253 K. The crystals were mounted on glass fibers, and the diffraction measurements were performed with a Nonius Kappa CCD area-detector diffractometer with Mo-$K\alpha$ radiation (λ = 0.71073 Å). The structures were solved by direct methods and refined by least-squares techniques on weighted F^2 values for all reflections (SHELXTL, 6.14).[20] All non-hydrogen atoms were assigned anisotropic displacement parameters and refined without positional constraints. All hydrogen atoms, including those involved in hydrogen bonding, were calculated with a riding model. Complex neutral-atom scattering factors were used. Compounds **2b**, **2d**, **4c**, and **6a** were crystallized with water molecules, whose H atoms could not be located. The crystal of compound **3a** diffracted very poorly. Attempts to get better crystals were unfruitful. The H atoms corresponding to the OH bridges could not be located in a difference Fourier map. The program SQUEEZE, a part of the Platon[21] package of crystallographic software, was used to calculate the solvent disorder area and remove its contribution to the overall intensity data.

X-ray crystal structure data for compounds **2b−e**, **3a**, **4a,c,d**, **5a,b**, and **6a,b** are included in the Supporting Information.

Synthesis of $[Pd_2\{\mu\text{-}(C_6H_4)PPh_2\}_2\{\mu\text{-}(R,R'_2pz)\}_2]$ (R = R′ = H (2a); R = Br; R′ = H (2b); and R = CH_3; R′ = H (2c)). The reaction of the corresponding pyrazole (0.112 mmol) with potassium hydroxide (0.112 mmol) dissolved in the minimum amount of methanol allowed us to obtain the corresponding potassium pyrazolate that was added to $[Pd_2\{\mu\text{-}(C_6H_4)PPh_2\}_2(NCMe)_4](BF_4)_2$ obtained by a reaction of a suspension of $[Pd_4(\mu\text{-}Br)_4\{\mu\text{-}(C_6H_4)PPh_2\}_4]$ (**1**) (50 mg, 0.028 mmol) in 20 mL of CH_2Cl_2/NCMe (8/1) with $AgBF_4$ (22 mg, 0.112 mmol). After 5 min of stirring, the solution was evaporated to dryness. The yellow crude product obtained was extracted with dichloromethane, filtered over a short plug of silica, and precipitated by the addition of hexane to give a yellow microcrystalline powder which was collected by filtration and washed with hexane.

Yield: 48 mg (98%) (**2a**); 32 mg (64%) (**2b**); 39 mg (78%) (**2c**).

Characterization Data for ***2a***. ^{1}H NMR (CD_2Cl_2, 400 MHz, 298 K) δ 7.75 (m, 2H, ar), 7.40 (m, 2H, ar), 7.34 (m, 8H, ar), 7.20 (m, 2H, ar), 7.15 (d, J = 2 Hz, 2H, py), 6.99 (m, 4H, ar), 6.85 (m, 2H, ar), 6.73 (m, 8H, ar), 6.24 (d, J = 2 Hz, 2H, py), 5.58 (s, 2H, py); ^{31}P NMR

DOI: 10.1021/acs.inorgchem.5b02506
Inorg. Chem. XXXX, XXX, XXX−XXX

(CD_2Cl_2, 161 MHz, 298 K) δ 37.4 (s); ^{13}C NMR (CD_2Cl_2, 100.6 MHz, 298 K) δ 160.4 (d, J = 32 Hz, C metalated), 140.0−122.4 (ar, py), 104.2 (s, py). Anal. Calcd for $C_{42}H_{34}N_4P_2Pd_2$: C, 58.01; H, 3.94; N, 6.44. Found: C, 58.58; H, 3.75; N, 6.01.

Characterization Data for ***2b***. ^1H NMR (CD_2Cl_2, 400 MHz, 298 K) δ 7.72 (m, 2H, ar), 7.44 (m, 2H, ar), 7.37 (m, 4H, ar), 7.25 (m, 6H, ar), 7.13 (s, 2H, py), 7.03 (m, 4H, ar), 6.95 (m, 2H, ar), 6.82 (m, 2H, ar), 6.74 (m, 6H, ar), 6.08 (s, 2H, py); ^{31}P NMR (CD_2Cl_2, 161 MHz, 298 K) δ 37.7 (s); ^{13}C NMR (CD_2Cl_2, 100.6 MHz, 298 K) δ 162.6 (d, J = 29 Hz, C metalated), 140.0−122.9 (ar, py), 90.5 (s, py). Anal. Calcd for $C_{42}H_{32}Br_2N_4P_2Pd_2$: C, 49.10; H, 3.14; N 5.45. Found: C, 49.62; H, 2.97; N, 4.86.

Characterization Data for ***2c***. ^1H NMR (CD_2Cl_2, 400 MHz, 298 K) δ 7.71 (m, 2H, ar), 7.34 (m, 2H, ar), 7.29 (m, 4H, ar), 7.20 (m, 6H, ar), 6.97 (m, 4H, ar), 6.91 (s, 2H, py), 6.87 (m, 2H, ar), 6.71 (m, 8H, ar), 5.89 (s, J = 2 Hz, 2H, py), 1.60 (s, 6H, CH_3); ^{31}P NMR (CD_2Cl_2, 161 MHz, 298 K) δ 37.5 (s); ^{13}C NMR (CD_2Cl_2, 100.6 M Hz, 298 K) δ 164.9 (d, J = 31 Hz, C metalated), 147.2−122.5 (ar, py), 114.0 (s, py), 9.0 (s, CH_3). Anal. Calcd for $C_{44}H_{38}N_4P_2Pd_2$: C, 58.88; H, 4.27; N, 6.24. Found: C, 58.62; H, 4.14; N, 6.01.

Synthesis of the Silver Pyrazolates, Ag(3,5-Me_2pz) and Ag(4-Br,3,5-Me_2pz). In a 1:1 stoichiometric ratio, a solution of $AgNO_3$ (2 mmol) in water (1 mL) was added under vigorous stirring to a CH_2Cl_2 solution (2 mL) of the corresponding pyrazole (2 mmol) previously deprotonated with a methanolic solution of KOH. In each case, a white precipitate was obtained that was filtered, washed with MeOH (2 × 4 mL), and vacuum-dried. They were used without further purification. Yields: Ag(3,5-Me_2pz) 360 mg (89%); Ag(4-Br,3,5-Me_2pz) 433 mg (77%).

Synthesis of $[Pd_2\{\mu\text{-}(C_6H_4)PPh_2\}_2\{\mu\text{-}(R,R'_2pz)\}_2]$ (R = H; R′ = CH_3 (2d) and R = Br, R′ = CH_3 (2e)). To a suspension of $[Pd_4(\mu\text{-}Br)_4\{\mu\text{-}(C_6H_4)PPh_2\}_4]$ (**1**) (50 mg, 0.028 mmol) in CH_2Cl_2 (10 mL) was added the corresponding silver pyrazolate (0.115 mmol). After 24 h of stirring, the crude was filtered over a short plug of silica, and the solution was evaporated to dryness and precipitated by the addition of hexane to give a yellow microcrystalline powder, which was collected by filtration and washed with hexane.

Yield: 41 mg (79%) (**2d**) ; 48 mg (79%) (**2e**).

Characterization Data for ***2d***. ^1H NMR (CD_2Cl_2, 400 MHz, 298 K) δ 8.01 (m, 2H, ar), 7.15 (m, 16H, ar), 6.93 (m, 2H, ar), 6.73 (s, 4H, ar), 6.54 (m, 4H, ar), 5.37 (s, 2H, py), 2.12 (s, 6H, CH_3) 1.43 (s, 6H, CH_3); ^{31}P NMR (CD_2Cl_2, 161 MHz, 298 K) δ 34.4 (s); ^{13}C NMR (CD_2Cl_2, 100.6 M Hz, 298 K) δ 167.5 (d, J = 32 Hz, C metalated), 146.8−121.6 (ar, py), 102.4 (s, py), 12.9 (s, CH_3), 12.3 (s, CH_3). Anal. Calcd for $C_{46}H_{42}N_4P_2Pd_2$: C, 59.69; H, 4.57; N, 6.05. Found: C, 59.45; H, 4.51; N, 6.15.

Characterization Data for ***2e***. ^1H NMR (CD_2Cl_2, 400 MHz, 298 K) δ 7.95 (m, 2H, ar), 7.27 (m, 2H, ar), 7.13 (m, 14H, ar), 6.94 (m, 2H, ar), 6.72 (m, 4H, ar), 6.58 (s, 4H, ar), 2.09 (s, 6H, CH_3), 1.31 (s, 6H, CH_3); ^{31}P NMR (CD_2Cl_2, 161 MHz, 298 K) δ 35.4 (s); ^{13}C NMR (CD_2Cl_2, 100.6 M Hz, 298 K) δ 165.8 (d, J = 31 Hz, C metalated), 145.1−122.0 (ar), 89.8 (s, py), 11.9 (s, CH_3), 11.2 (s, CH_3). Anal. Calcd for $C_{46}H_{40}Br_2N_4P_2Pd_2$: C, 50.99; H, 3.72; N, 5.17. Found: C, 50.85; H, 3.57; N, 5.01.

Synthesis of $[Pd_2\{\mu\text{-}(C_6H_4)PPh_2\}_2Br_2(R,R'_2pzH)_2]$ (R = R′= H (4a); R = Br, R′ = H (4b); R = CH_3, R′ = H (4c); R = H, R′ = CH_3 (4d); and R = Br, R′ = CH_3 (4e). To a suspension of $[Pd_4(\mu\text{-}Br)_4\{\mu\text{-}(C_6H_4)PPh_2\}_4]$ (**1**) (50 mg, 0.028 mmol) in CH_2Cl_2 (10 mL) was added the corresponding pyrazole in a 1:4 molar ratio. The solution was stirred for 4 h, evaporated to dryness, and precipitated by the addition of hexane to give a yellow powder, which was collected by filtration and washed with hexane.

Yield: 47 mg (82%) (**4a**); 59 mg (89%) (**4b**); 47 mg (80%) (**4c**); 55 mg (91%) (**4d**); 67 mg (96%) (**4e**).

Characterization Data for ***4a***. ^1H NMR (CD_2Cl_2, 400 MHz, 298 K) δ 12.01 (s, 2H, NH), 8.05 (m, 2H, py), 7.21 (m, 2H, ar), 7.12 (m, 12H, ar), 7.04 (m, 4H, ar), 6.78 (m, 8H, ar), 6.73 (m, 4H, ar, py), 6.11 (m, 2H, py); ^{31}P NMR (CD_2Cl_2, 161 MHz, 298 K) δ 18.7 (s); ^{13}C NMR (CD_2Cl_2, 100.6 MHz, 298 K) δ 159.5 (t, J = 12 Hz, metalated), 141.6 (s, py), 141.0−122.5 (ar, py), 104.8 (s, py). Anal. Calcd for $C_{42}H_{36}Br_2N_4P_2Pd_2$: C, 48.91; H, 3.52; N, 5.43. Found: C, 48.23; H, 3.92; N, 5.05.

Characterization Data for ***4b***. ^1H NMR (CD_2Cl_2, 400 MHz, 298 K) δ 12.22 (s, 2H, NH), 8.04 (d, J = 2 Hz, 2H, py), 7.36 (m, 2H, ar), 7.28 (s, 2H, ar), 7.14 (m, 14H, ar), 6.90 (m, 4H, ar), 6.84 (m, 4H, ar), 6.78 (d, J = 2 Hz, 2H, py), 6.72 (m, 2H, ar); ^{31}P NMR (CD_2Cl_2, 161 MHz, 298 K) δ 18.9 (s); ^{13}C NMR (CD_2Cl_2, 100.6 MHz, 298 K) δ 158.6 (t, J = 12 Hz, metalated), 142.1 (s, py), 140.8−122.0 (ar, py), 92.9 (s, py). Anal. Calcd for $C_{42}H_{34}Br_4N_4P_2Pd_2$: C, 42.42; H, 2.88; N, 4.71. Found: C, 42.87; H, 3.05; N, 4.56.

Characterization Data for ***4c***. ^1H NMR (CD_2Cl_2, 400 MHz, 298 K) δ 11.64 (s, 2H, NH), 7.70 (s, 2H, py), 7.22 (m, 2H, ar), 7.07 (m, 4H. ar), 7.02 (m, 8H, ar), 6.93 (m, 4H, ar), 6.74 (m, 8H, ar), 6.59 (m, 2H, ar), 6.40 (s, 2H, py), 1.88 (s, 6H, CH_3); ^{31}P NMR (CD_2Cl_2, 161 MHz, 298 K) δ 18.7 (s); ^{13}C NMR (CD_2Cl_2, 100.6 MHz, 298 K) δ 159.8 (t, J = 12 Hz, metalated), 141.4 (s, py), 141.1−122.5 (ar, py), 115.4 (s, py), 8.4 (s, CH_3). Anal. Calcd for $C_{44}H_{40}Br_2N_4P_2Pd_2$: C, 49.88; H, 3.81; N, 5.29. Found: C, 50.23; H, 3.46; N, 4.91.

Characterization Data for ***4d***. ^1H NMR (CD_2Cl_2, 400 MHz, 298 K) δ 11.90 (s, 2H, NH), 7.40 (s, 2H, ar), 7.35 (m, 2H, ar), 7.22 (m, 8H, ar), 7.16 (m, 2H, ar), 7.10 (m, 4H, ar), 7.03 (m, 4H, ar), 6.75 (m, 4H, ar), 6.63 (m, 2H, ar), 5.66 (s, 2H, py), 2.73 (s. 6H, CH_3), 1.88 (s, 6H, CH_3); ^{31}P NMR (CD_2Cl_2, 161 MHz, 298 K) δ 21.2 (s); ^{13}C NMR (CD_2Cl_2, 100.6 MHz, 298 K) δ 160.8 (t, J = 13 Hz, metalated), 141.4 (s, py), 141.1−122.5 (ar, py), 115.4 (s, py), 8.4 (s, CH_3). Anal. Calcd for $C_{46}H_{44}Br_2N_4P_2Pd_2$: C, 50.81; H, 4.08; N, 5.15. Found: C, 50.67; H, 4.22; N, 5.04.

Characterization Data for ***4e***. ^1H NMR (CD_2Cl_2, 400 MHz, 298 K) δ 12.08 (s, 2H, NH), 7.30 (m, 2H, ar), 7.23 (m, 2H, ar), 7.08 (m, 6H, ar), 7.01 (m, 4H, ar), 6.91 (m, 8H, ar), 6.70 (m, 2H, ar), 6.64 (m, 2H, ar), 6.49 (m, 2H, ar), 2.65 (s, 6H, CH_3), 1.63 (s, 6H, CH_3); ^{31}P NMR (CD_2Cl_2, 161 MHz, 298 K) δ 20.7 (s); ^{13}C NMR (CD_2Cl_2, 100.6 MHz, 298 K) δ 160.0 (t, J = 13 Hz, metalated), 146.7 (s, py), 140.5−122.5 (ar, py), 95.0 (s, py), 15.0 (s, CH_3), 9.5 (s, CH_3). Anal. Calcd for $C_{46}H_{42}Br_4N_4P_2Pd_2$: C, 44.37; H, 3.40; N, 4.50. Found: C, 44.02; H, 3.47; N, 4.84.

Synthesis of $[Pd_2\{\mu\text{-}(C_6H_4)PPh_2\}_2\{\mu\text{-}(R,R'_2pz\text{-}Ag\text{-}R,R'_2pz)\}_2]$ (R = R′ = H (5a); R = Br; R′ = H (5b); and R = CH_3; R′ = H (5c)). To a suspension of $[Pd_4(\mu\text{-}Br)_4\{\mu\text{-}(C_6H_4)PPh_2\}_4]$ (**1**) (30 mg, 0.017 mmol) in CH_2Cl_2 (10 mL) was added the corresponding silver pyrazolate in a 1:8.5 molar ratio (0.145 mmol). After 24 h of stirring, the crude was filtered over a short plug of silica, and the solution was evaporated to dryness and precipitated by the addition of hexane to give a white powder, which was collected by filtration and washed with hexane.

Yield: 20 mg (48%) (**5a**); 37 mg (71%) (**5b**) and 36 mg (83%) (**5c**).

Compound **5b** was also synthesized using the following procedure: to a suspension of $[Pd((C_6H_4)PPh_2)Br]_4$ (**1**) (30 mg, 0.017 mmol) in 10 mL of CH_2Cl_2/CH_3CN was added $AgBF_4$ (14 mg, 0.071 mmol). After 30 min of stirring, the solution was filtered, and 4-bromo-1*H*-pyrazole (12 mg, 0.146 mmol) was added. The solution was stirred for 1 h, and NEt_3 (1 mL) and AgBF4 (14 mg, 0.071 mmol) were added. After 24 h of stirring, the solution was evaporated to dryness. The yellow crude product obtained was extracted with dichloromethane, filtered over a short plug of silica, and precipitated by the addition of hexane to give a yellow microcrystalline powder, which was collected by filtration and washed with hexane. Yield: 20 mg (38%).

Characterization Data for ***5a***. ^1H NMR (CD_2Cl_2, 400 MHz, 298 K) δ 8.09 (d, J = 7 Hz, 2H, ar), 7.89 (m, 4H, ar), 7.58 (s, 2H, py), 7.45 (m, 6H, ar), 7.33 (m, 4H, ar, py), 7.01 (m, 2H, ar), 6.93 (m, 2H, ar), 6.72 (m, 6H, ar, py), 6.50 (m, 4H, ar), 6.17 (d, J = 2 Hz, 2H, py), 6.09 (s, 2H, py), 5.85 (m, 4H); ^{31}P NMR (CD_2Cl_2, 161 MHz, 298 K) δ 19.4 (s); ^{13}C NMR (CD_2Cl_2, 100.6 MHz, 298 K) δ 161.0 (d, J = 15 Hz, metalated), 140.0−122.5 (ar), 103.9 (s, py), 103.8 (s, py), 102.1 (s, py), 102.0 (s, py). Anal. Calcd for $C_{48}H_{40}Ag_2N_8P_2Pd_2$: C, 47.28; H, 3.31; N, 9.19. Found: C, 46.88; H, 3.04; N, 8.83.

Characterization Data for ***5b***. ^1H NMR (CD_2Cl_2, 400 MHz, 298 K) δ 8.04 (m, 2H, ar), 7.93 (m, 4H, py), 7.55 (d, J = 2 Hz, 2H, py), 7.50 (m, 6H, ar), 7.36 (s, 4H, ar), 7.02 (m, 4H, ar), 6.76 (m, 4H, ar),

DOI: 10.1021/acs.inorgchem.5b02506
Inorg. Chem. XXXX, XXX, XXX−XXX

6.71 (s, 2H, py), 6.62 (m, 4H, ar), 5.95 (m, 4H); ^{31}P NMR (CD_2Cl_2, 161 MHz, 298 K) δ 19.1 (s); ^{13}C NMR (CD_2Cl_2, 100.6 MHz, 298 K) δ 158.7 (d, J = 14 Hz, metalated), 140.0−122.5 (ar), 92.0 (s, py), 91.9 (s, py), 90.7 (s, py), 90.6 (s, py). Anal. Calcd for $C_{48}H_{36}Ag_2Br_4N_8P_2Pd_2$: C, 37.56; H, 2.36; N, 7.30. Found: C, 37.41; H, 2.15; N, 7.65.

Characterization Data for ***5c***. ^{1}H NMR (CD_2Cl_2, 400 MHz, 298 K) δ 8.12 (m, 2H, ar), 8.00 (m, 4H, ar), 7.47 (m, 6H, ar), 7.37 (s, 2H, py), 7.18 (s, 2H, py), 7.11 (s, 2H, py), 6.94 (m, 4H, ar), 6.68 (m, 4H, ar), 6.49 (m, 6H, ar, py), 5.80 (m, 4H, ar), 2.06 (s, 6H, CH_3), 2.02 (s, 6H, CH_3); ^{31}P NMR (CD_2Cl_2, 161 MHz, 298 K) δ 19.5 (s); ^{13}C NMR (CD_2Cl_2, 100.6 MHz, 298 K) δ 160.9 (d, J = 15 Hz, metalated), 140.1−122.5 (ar), 114.3 (s, py), 114.2 (s, py), 112.5 (s, py), 112.4 (s, py), 8.9 (s, CH_3), 8.8 (s, CH_3. Anal. Calcd for $C_{52}H_{48}Ag_2N_8P_2Pd_2$: C, 48.96; H, 3.79; N, 8.78. Found: C, 49.22; H, 4.03; N, 8.96.

Synthesis of $[Pd_2\{\mu\text{-}(C_6H_4)PPh_2\}_2\{\mu\text{-}(R,R'_2pz)\}_2Cl_2]$ (R = R′ = H (6a) and R = Br, R′ = H (6b)). To a solution at 223 K of **2a** (50 mg, 0.058 mmol) or **2b** (50 mg, 0.052 mmol) in CH_2Cl_2 (5 mL) was added iodobenzene dichloride, 17 mg (0.062 mmol) or 15 mg (0.055 mmol), respectively. The solution immediately changed from yellow to red. After 5 min of stirring, the solution was evaporated to dryness, and hexane was added. The red microcrystalline precipitate obtained was isolated by filtration and washed with cold hexane. Yield: 31 mg (57%) (**6a**); 39 mg (68%) (**6b**).

Characterization Data for ***6a***. ^{1}H NMR (CD_2Cl_2, 400 MHz, 223 K) δ 8.53 (dd, J = 8 Hz, J = 4 Hz, 2H, ar), 7.56 (m, 4H, ar), 7.39 (m, 10H, ar, py), 7.18 (m, 4H, ar), 7.03 (m, 6H, ar), 6.83 (m, 2H, ar), 6.75 (d J = 3 Hz, 2H, py), 6.53 (m, 2H, ar), 5.82 (d, J = 3 Hz, 2H, py); ^{31}P NMR (CD_2Cl_2, 161 MHz, 298 K) δ 17.3 (s); ^{13}C NMR (CD_2Cl_2, 100.6 MHz, 298 K) δ 159.7 (dd, J = 17 Hz, J = 3 Hz, metalated), 138.8−124.5 (ar), 106.9 (s, py).

Characterization Data for ***6b***. ^{1}H NMR (CD_2Cl_2, 400 MHz, 223 K) δ 8.33 (m, 2H, ar), 7.54 (m, 6H, ar), 7.45 (m, 4H, ar), 7.34 (m, 6H, ar, py), 7.26 (m, 4H, ar), 7.17 (m, 4H, ar), 6.98 (m, 2H, ar), 6.88 (m, 2H, ar), 6.53 (s, 2H, py); ^{31}P NMR (CD_2Cl_2, 161 MHz, 298 K) δ 18.2 (s); ^{13}C NMR (CD_2Cl_2, 100.6 MHz, 298 K) δ 158.5 (dd, J = 17 Hz, J = 3 Hz, metalated), 139.0−124.8 (ar, py), 93.0 (s, py).

Computational Details. All molecular compounds were fully optimized with the Gaussian 09 program package[22] at the DFT level of theory. A hybrid density functional B3PW91[23] was utilized together with the basis set consisting of the Stuttgart−Dresden effective core potential with an additional p-polarization function for Pd atoms (SDD(p)),[24] def2-TZVPPD[25] effective core potential with triple-ζ-valence basis set with two sets of polarization, and diffuse basis functions for Ag atoms and the standard all-electron basis set 6-31G(d) for all other atoms. Frequency calculations with no scaling were conducted to ensure optimization to true minima. None of the optimized structures gave imaginary frequencies. Moreover, the absorption properties in dichloromethane (CH_2Cl_2) media were calculated by TD-DFT[26] with the conductor-like polarized continuum model (CPCM) for the solvent effects.[27]

Topological charge density analysis was performed with the QTAIM[28] methods, which allowed us to access the nature of the bonding via calculating different properties of the electron density at the BCPs. The analysis was done with the AIMAll program[29] using the wave functions obtained from the DFT calculations with the computationally fully optimized structures.

■ ASSOCIATED CONTENT

Ⓢ Supporting Information

The Supporting Information is available free of charge on the ACS Publications website at DOI: 10.1021/acs.inorgchem.5b02506.

Perspective view of compounds **2b** and **2e**; stereochemistry of compounds **2**; comparison of the simulated spectra obtained from TD-DFT calculations (Calculated) and the experimental UV−vis spectra (Experimental); comparison of frontier molecular orbitals involved in the lowest energy excitation, HOMO (left) and LUMO+1 (right), of the palladium(II) compound **2a**; weak interactions of the solvent of crystallization (CH_2Cl_2) with the pyrazolate rings in compound **2c**; perspective view of compounds **4c** and **4d**; stereochemistry for compounds **4**; optimized structure of the palladium(II) pyrazolate complex **4a** showing the results of the topological charge density analysis at the Br···H−N_{pz} BCP; stereochemistry for compounds **5**; stereochemistry and torsion angles for compounds **2b−e**; properties of the electron density at the M-M′ (where M, M′ = Pd or Ag) BCP according to the QTAIM analysis of the solved palladium-pyrazolato structures; dihedral angle between the planes containing the Pd-N-N-Pd fragments for compounds **2a−e** and **6a,b**; dihedral angle formed by the best least-squares coordination planes of the metals for compounds **2b−e**, **4a,a′,c,d**, and **5a,b**; bow angles between the planes defined by N1-N2-N1-N2 and N1-Pd-N2 for compounds **2b−e** and **6a,b**; relevant conformational features for compounds **2b−e** and **6a,b**; stereochemistry and torsion angles for compounds **4a,a′,c,d**, **5a,b**, and **6a,b**; X-ray crystal structure data for compounds **2b−e**, **3a**, **4a,c,d**, **5a,b**, and **6a,b** (PDF)

Cartesian coordinates of all the optimized geometries of **1**, **2a−e**, **3a−e**; **4a−e**, **5a−e**, and **6a,b** (PDF)

X-ray crystal structure data for compounds **2b−e**, **3a**, **4a,c,d**, **5a,b**, and **6a,b** in CIF format (ZIP)

■ AUTHOR INFORMATION

Corresponding Authors

*(P.H.) E-mail: pipsa.hirva@uef.fi.

*(M.A.U.) E-mail: angeles.ubeda@uv.es.

Notes

The authors declare no competing financial interest.

■ ACKNOWLEDGMENTS

We are grateful to SCSIE of the Universitat de València for instrumental support. Financial support provided by the Inorganic Materials Chemistry Graduate Program (EMTKO) and the strategic funding of the University of Eastern Finland are gratefully acknowledged (A.O.). The computational work has been facilitated by the use of the Finnish Grid Infrastructure resources.

■ REFERENCES

(1) (a) Trofimenko, S. *Chem. Rev.* **1972**, *72*, 497−509. (b) Trofimenko, S. *Prog. Inorg. Chem.* **1986**, *34*, 115−210. (c) Sadimenko, A. P.; Basson, S. S. *Coord. Chem. Rev.* **1996**, *147*, 247−297. (d) La Monica, G.; Ardizzoia, G. A. *Prog. Inorg. Chem.* **1997**, *46*, 151−238. (e) Mukherjee, R. *Coord. Chem. Rev.* **2000**, *203*, 151−170. (f) Sadimenko, A. P. *Adv. Heterocycl. Chem.* **2001**, *80*, 157−240.

(2) Röder, J. C.; Meyer, F.; Kaifer, E.; Pritzkow, H. *Eur. J. Inorg. Chem.* **2004**, *2004*, 1646−1660.

(3) Yu, S.-Y; Li, S.-H; Huang, H.-P; Zhang, Z.-X; Jiao, Q.; Shen, H.; Hu, X.-X; Huang, H. *Curr. Org. Chem.* **2005**, *9*, 555−563.

(4) (a) Ara, I.; Falvello, L. R.; Forniés, J.; Lasheras, R.; Martín, A.; Oliva, O.; Sicilia, V. *Inorg. Chim. Acta* **2006**, *359*, 4574−4584. (b) Ara, I.; Forniés, J.; Lasheras, R.; Martín, A.; Sicilia, V. *Eur. J. Inorg. Chem.* **2006**, *2006*, 948−957. (c) Boixassa, A.; Pons, J.; Solans, X.; Font-Badía, M.; Ros, J. *Inorg. Chem. Commun.* **2003**, *6*, 922−925. (d) Umakoshi, K.; Yamauchi, Y.; Nakamiya, K.; Kojima, T.; Yamasaki, M.; Kawano, H.; Onishi, M. *Inorg. Chem.* **2003**, *42*, 3907−3916. (e) Forniés, J.; Martín, A.; Sicilia, V.; Martín, L. F. *Chem. - Eur. J.* **2003**, *9*, 3427−3435. (f) Ardizzoia, G. A.; La Monica, G.;

DOI: 10.1021/acs.inorgchem.5b02506
Inorg. Chem. XXXX, XXX, XXX−XXX

Cenicni, S.; Moret, M.; Masciocchi, N. *J. Chem. Soc., Dalton Trans.* **1996**, 1351−1357.
(5) (a) Chaudhari, K. R.; Wadawale, A. P.; Kumar, M.; Jain, V. K. *J. Organomet. Chem.* **2014**, *760*, 55−59. (b) Colquhoun, V. P.; Schildbach, D.; Marin-Romo, R.; Strohmann, C.; Villafañe, F. *Eur. J. Inorg. Chem.* **2012**, *2012*, 3427−3434. (c) Santana, A. M.; Ferreira, J. G.; Moro, A. C.; Lemos, S. C.; Mauro, A. E.; Netto, A. V. G.; Frem, R. C. G.; Santos, R. H. A. *Inorg. Chem. Commun.* **2011**, *14*, 83−86. (d) Pérez, J.; Espinosa, A.; Galiana, J. M.; Pérez, E.; Serrano, J. L.; Aranda, M. A. G.; Insausti, M. *Dalton.Trans.* **2009**, 9625−9636. (e) Chakraborty, J.; Saha, M. K.; Banerjee, P. *Inorg. Chem. Commun.* **2007**, *10*, 671−676. (f) Huang, H.-P.; Liu, L.-X. *Acta Crystallogr., Sect. E: Struct. Rep. Online* **2007**, *63*, m1875−m1876. (g) Huang, H.-P.; Wu, Q.; Liu, X.-L.; Song, Q.-F. *Acta Crystallogr., Sect. E: Struct. Rep. Online* **2007**, *63*, m458−m459. (h) Singhal, A.; Mishra, R.; Kulshreshtha, S. K.; Bernhardt, P. V.; Tiekink, E. R. T. *J. Organomet. Chem.* **2006**, *691*, 1402−1410. (i) Chakraborty, J.; Mayer-Figge, H.; Sheldrick, W. S.; Banerjee, P. *Polyhedron* **2006**, *25*, 3138−3144. (j) Huang, H.-P.; Li, S.-H.; Yu, S.-Y.; Li, Y.-Z.; Jiao, Q.; Pan, Y.-J. *Inorg. Chem. Commun.* **2005**, *8*, 656−660. (k) Wang, Z.; Abernethy, C. D.; Cowley, A. H.; Jones, J. N.; Jones, R. A.; Macdonald, C. L. B.; Zhang, L. *J. Organomet. Chem.* **2003**, *666*, 35−42. (l) Pons, J.; Chadghan, A.; Casabo, J.; Alvarez-Larena, A.; Piniella, J. F.; Ros, J. *Inorg. Chem. Commun.* **2000**, *3*, 296−299.
(6) (a) Umakoshi, K.; Kojima, T.; Arikawa, Y.; Onishi, M. *Chem. - Eur. J.* **2006**, *12*, 5094−5104. (b) Umakoshi, K.; Kojima, T.; Saito, K.; Akatsu, S.; Onishi, M.; Ishizaka, S.; Kitamuta, N.; Nakao, Y.; Sakaki, S.; Ozawa, Y. *Inorg. Chem.* **2008**, *47*, 5033−5035.
(7) (a) Powers, D. C.; Ritter, T. *Top. Organomet. Chem.* **2011**, *35*, 129−156. (b) Mirica, L. M.; Khusnutdinova, J. R. *Coord. Chem. Rev.* **2013**, *257*, 299−314.
(8) Cotton, F. A.; Gu, J.; Murillo, C. A.; Timmons, D. J. *J. Am. Chem. Soc.* **1998**, *120*, 13280−13281.
(9) (a) Cotton, A. F.; Koshevoy, I. O.; Lahuerta, P.; Murillo, C. A.; Sanaú, M.; Úbeda, M. A.; Zhao, Q. *J. Am. Chem. Soc.* **2006**, *128*, 13674−13679. (b) Penno, D.; Lillo, V.; Koshevoy, I. O.; Sanaú, M.; Úbeda, M. A.; Lahuerta, P.; Fernández, E. *Chem. - Eur. J.* **2008**, *14*, 10648−10655. (c) Penno, D.; Estevan, E.; Fernández, F.; Hirva, P.; Lahuerta, P.; Sanaú, M.; Úbeda, M. A. *Organometallics* **2011**, *30*, 2083−2094. (d) Ibañez, S.; Estevan, F.; Hirva, P.; Sanaú, M.; Úbeda, M. A. *Organometallics* **2012**, *31*, 8098−8108. (e) Ibañez, S.; Vrečko, D. N.; Estevan, F.; Hirva, P.; Sanaú, M.; Úbeda, M. A. *Dalton Trans.* **2014**, *43*, 2961−2970. (f) Ibañez, S.; Oresmaa, L.; Estevan, F.; Hirva, P.; Sanaú, M.; Úbeda, M. A. *Organometallics* **2014**, *33*, 5378−5391. (g) Estevan, F.; Ibañez, S.; Ofori, A.; Hirva, P.; Sanaú, M.; Úbeda, M. A. *Eur. J. Inorg. Chem.* **2015**, *2015*, 2822−2832.
(10) (a) Powers, D. C.; Ritter, T. *Nat. Chem.* **2009**, *1*, 302−309. (b) Powers, D. C.; Geibel, M. A. L.; Kein, J. E. M. N.; Ritter, T. *J. Am. Chem. Soc.* **2009**, *131*, 17050−17051. (c) Chuang, G. J.; Wang, W.; Lee, E.; Ritter, T. *J. Am. Chem. Soc.* **2011**, *133*, 1760−1762.
(11) Campbell, M. G.; Powers, D. C.; Raynaus, J.; Graham, M. J.; Xie, P.; Lee, E.; Ritter, T. *Nat. Chem.* **2011**, *3*, 949−953.
(12) Powers, D. C.; Ritter, T. *Organometallics* **2013**, *32*, 2042−2045.
(13) (a) Cotton, F. A.; Murillo, C. A. *Eur. J. Inorg. Chem.* **2006**, *2006*, 4209−4218. (b) Koshevoy, I. O.; Lahuerta, P.; Sanaú, M.; Úbeda, M. A.; Doménech, A. *Dalton Trans.* **2006**, 5536−5541.
(14) (a) Scheuermann, M. L.; Boyce, D. W.; Grice, K. A.; Kaminsky, W.; Stoll, S.; Tolman, W. B.; Swang, O.; Goldberg, K. I. *Angew. Chem., Int. Ed.* **2014**, *53*, 6492−6495. (b) Egbert, J. D.; Chartoire, A.; Slawin, A. M. Z.; Nolan, S. P. *Organometallics* **2011**, *30*, 4494−4496. (c) Cross, W. B.; Daly, C. G.; Ackerman, R. L.; George, I. R.; Singh, K. *Dalton Trans.* **2011**, *40*, 495−505. (d) Bettucci, L.; Bianchini, C.; Oberhauser, W.; Hsiao, T.-H.; Lee, H. M. *J. Mol. Catal. A: Chem.* **2010**, *322*, 63−72. (e) Ortiz, A. L.; Cumbrera, F. L.; Pérez, J.; Meléndez-Martínez, J. J.; Palatinus, L. *J. Alloys Compd.* **2009**, *467*, 322−326. (f) Pérez, J.; Espinosa, A.; Galiana, J. M.; Pérez, E.; Serrano, J. L.; Cabeza, A.; Aranda, A. G. *Eur. J. Inorg. Chem.* **2008**, *2008*, 3687−3697. (g) Hadzovic, A.; Song, D. *Inorg. Chem.* **2008**, *47*, 12010−12017. (h) Adrian, R. A.; Broker, G. A.; Tiekink, E. R. T.; Walmsley, J. A. *Inorg. Chim. Acta* **2008**, *361*, 1261−1266. (i) Bercaw, J. E.; Hazari, N.; Labinger, J. A.; Oblad, P. F. *Angew. Chem., Int. Ed.* **2008**, *47*, 9941−9943. (j) Nama, D.; Pregosin, P. S.; Albinati, A.; Rizzato, S. *Organometallics* **2007**, *26*, 2111−2121. (k) Pérez, J.; Serrano, J. L.; Galiana, J. M.; Cumbrera, F. L.; Ortiz, A. L.; Sánchez, G.; García, J. *Acta Crystallogr., Sect. B: Struct. Sci.* **2007**, *63*, 75−80. (l) Zhao, B.; Lu, X. *Org. Lett.* **2006**, *8*, 5987−5990. (m) Adrian, R. A.; Benson, R. E.; Daniels, L. M.; Tiekink, E. R. T.; Walmsley, J. A. *Acta Crystallogr., Sect. E: Struct. Rep. Online* **2006**, *62*, m601−m603. (n) Shen, W. Z.; Gupta, D.; Lippert, B. *Inorg. Chem.* **2005**, *44*, 8249−8258. (o) Serrano, J. L.; Fairlamb, I. J. S.; Sánchez, G.; García, L.; Pérez, J.; Vives, J.; López, G.; Crawforth, C. M.; Taylor, R. J. K. *Eur. J. Inorg. Chem.* **2004**, *2004*, 2706−2715. (p) Ackerman, L. A.; Sadighi, J. P.; Kurtz, D. M.; Labinger, J. A.; Bercaw, J. E. *Organometallics* **2003**, *22*, 3884−3890. (q) Getty, A. D.; Goldberg, K. I. *Organometallics* **2001**, *20*, 2545−2551. (r) Grushin, V. V.; Alper, H. *Organometallics* **1993**, *12*, 1890−1901. (s) Kannan, S.; James, A. J.; Sharp, P. R. *Polyhedron* **2000**, *19*, 155−163. (t) Schnebeck, R.-D.; Freisinger, E.; Lippert, B. *Eur. J. Inorg. Chem.* **2000**, *2000*, 1193−1200. (u) Fujii, A.; Hagiwara, E.; Sodeoka, M. *J. Am. Chem. Soc.* **1999**, *121*, 5450−5458. (v) Ogoshi, S.; Tsutsumi, K.; Shinagawa, K.; Kurosawa, H. *Chem. Lett.* **1999**, 123−124. (w) Pieri, G.; Pasquali, M.; Leoni, P.; Englert, U. *J. Organomet. Chem.* **1995**, *491*, 27−30. (x) López, G.; Ruiz, J.; García, G.; Vicente, C.; Casabó, J.; Molins, E.; Miratvilles, C. *Inorg. Chem.* **1991**, *30*, 2605−2610. (y) Pisano, C.; Consiglio, G.; Sironi, A.; Moret, M. *J. Chem. Soc., Chem. Commun.* **1991**, 421−423.
(15) (a) Fulmer, G. R.; Kaminsky, W.; Kemp, R. A.; Goldberg, K. I. *Organometallics* **2011**, *30*, 1627−1636. (b) Cao, L.; Jennings, M. C.; Puddephatt, R. J. *Dalton Trans.* **2009**, 5171−5176. (c) Yang, Y.; Miao, R.; Li, Y.; Hong, J.; Zhao, C.; Guo, Z.; Zhu, L. *Dalton Trans.* **2005**, 1613−1619. (d) Klein, A.; Dogan, A.; Feth, M.; Bertagnolli, H. *Inorg. Chim. Acta* **2003**, *343*, 189−201.
(16) (a) Kapdi, A. R.; Dhangar, G.; Serrano, J. L.; Pérez, J.; García, L.; Fairlamb, I. J. S. *Chem. Commun.* **2014**, *50*, 9859−9861. (b) Wei, C. S.; Davies, G. H. M.; Soltani, O.; Albrecht, J.; Gao, Q.; Pathirana, C.; Hsiao, Y.; Tummala, S.; Eastgate, M. D. *Angew. Chem., Int. Ed.* **2013**, *52*, 5822−5826. (c) Hanley, P.; Hartwig, J. H. *J. Am. Chem. Soc.* **2011**, *133*, 15661−15673. (d) Wojaczynski, J.; Latos-Grazynski, L. *Chem. - Eur. J.* **2010**, *16*, 2679−2682. (e) Allscher, T.; Klüfers, P.; Labisch, O. *Carbohydr. Res.* **2007**, *342*, 1419−1426. (f) Benavente, R.; Espinet, P.; Martín-Álvarez, J. M.; Miguel, J. A.; Aullón, G. *Inorg. Chem.* **2007**, *46*, 2035−2040. (g) Adrian, R. A.; Zhu, S.; Powell, D. R.; Broker, G. A.; Tickink, E. R.; Walmsley, J. A. *Dalton Trans.* **2007**, 4399−4404. (h) Nama, D.; Schott, D.; Pregosin, P. S.; Veiros, L. F.; Calhorda, M. J. *Organometallics* **2006**, *25*, 4596−4604. (i) Chen, C.-L.; Liu, Y.-H.; Peng, S.-M.; Liu, S.-T. *J. Organomet. Chem.* **2004**, *689*, 1806−1815. (j) Kannan, S.; James, A. J.; Sharp, P. R. *Inorg. Chim. Acta* **2003**, *345*, 8−14. (k) O'Keef, B. J.; Steel, P. J. *Organometallics* **2003**, *22*, 1281−1292. (l) Miyaji, T.; Kujime, M.; Hikichi, S.; Moro-oka, Y.; Akita, M. *Inorg. Chem.* **2002**, *41*, 5286−5295. (m) Akita, M. A.; Miyaji, T.; Muroga, N.; Mock-Knoblauch, C.; Adam, W.; Hikichi, S.; Moro-oka, Y. *Inorg. Chem.* **2000**, *39*, 2096−2102. (n) Sánchez, G.; Serrano, J. L.; García, J.; López, G.; Pérez, J.; Molins, E. *Inorg. Chim. Acta* **1999**, *287*, 37−46. (o) Driver, M. S.; Hartwig, J. F. *Organometallics* **1997**, *16*, 5706−5715. (p) Apfelbacher, A.; Braunstein, P.; Brissieux, L.; Welter, R. *Dalton.Trans.* **2003**, 1669−1674. (q) Ruiz, J.; Rodriguez, V.; López, G.; Chaloner, P. A.; Hitchcock, P. B. *J. Chem. Soc., Dalton Trans.* **1997**, 4271−4276. (r) Driver, M. S.; Hartwig, J. F. *J. Am. Chem. Soc.* **1996**, *118*, 4206−4207.
(17) Masciocchi, N.; Moret, M.; Cairati, P.; Sironi, A.; Ardizzoia, G. A.; La Monica, G. *J. Am. Chem. Soc.* **1994**, *116*, 7668−7676.
(18) (a) Estevan, F.; García-Bernabé, A.; Lahuerta, P.; Sanaú, M.; Úbeda, M. A.; Ramírez de Arellano, M. C. *Inorg. Chem.* **2000**, *39*, 5964−5969. (b) Aarif, A. M.; Estevan, F.; García-Bernabé, A.; Lahuerta, P.; Sanaú, M.; Úbeda, M. A. *Inorg. Chem.* **1997**, *36*, 6472−6475.
(19) Lucas, H. J.; Kennedy, E. R. *Organic Synthesis*; Wiley&Sons: New York, 1955; Collect. Vol. *III*, p 482.
(20) *SHELXTL*, version 6;14; Brucker: Madison, WI, 2000.

DOI: 10.1021/acs.inorgchem.5b02506
Inorg. Chem. XXXX, XXX, XXX−XXX

(21) Spek, A. L. *Acta Crystallogr., Sect. D: Biol. Crystallogr.* **2009**, *65*, 148−155.
(22) Frisch, M. J.; Trucks, G. W.; Schlegel, H. B. Scuseria, G. E.; Robb, M. A.; Cheeseman, J. R.; Scalmani, G.; Barone, V.; Mennucci, B.; Petersson, G. A.; Nakatsuji, H.; Caricato, M.; Li, X.; Hratchian, H. P.; Izmaylov, A. F.; Bloino, J.; Zheng, G.; Sonnenberg, J. L.; Hada, M.; Ehara, M.; Toyota, K.; Fukuda, R.; Hasegawa, J.; Ishida, M.; Nakajima, T.; Honda, Y.; Kitao, O.; Nakai, H.; Vreven, T.; Montgomery, J. A.; Peralta, J. E., Jr.; Ogliaro, F.; Bearpark, M.; Heyd, J. J.; Brothers, E.; Kudin, K. N.; Staroverov, V. N.; Kobayashi, R.; Normand, J.; Raghavachari, K.; Rendell, A.; Burant, J. C.; Iyengar, S. S.; Tomasi, J.; Cossi, M.; Rega, N.; Millam, J. M.; Klene, M.; Knox, J. E.; Cross, J. B.; Bakken, V.; Adamo, C.; Jaramillo, J.; Gomperts, R.; Stratmann, R. E.; Yazyev, O.; Austin, A. J.; Cammi, R.; Pomelli, C.; Ochterski, J. W.; Martin, R. L.; Morokuma, K.; Zakrzewski, V. G.; Voth, G. A.; Salvador, P.; Dannenberg, J. J.; Dapprich, S.; Daniels, A. D.; Farkas, Ö.; Foresman, J. B.; Ortiz, J. V.; Cioslowski, J.; Fox, D. J. In *Gaussian 09*, revision C.01; Gaussian, Inc.: Wallingford, CT, 2009.
(23) (a) Perdew, J. P.; Wang, Y. *Phys. Rev. B: Condens. Matter Mater. Phys.* **1992**, *45*, 13244−13249. (b) Becke, A. D. J. *J. Chem. Phys.* **1993**, *98*, 5648−5652.
(24) Andrae, D.; Häussermann, U.; Dolg, M.; Stoll, H.; Preuss, H. *Theor. Chim. Acta* **1990**, *77*, 123−141.
(25) Rappoport, D.; Furche, F. *J. Chem. Phys.* **2010**, *133*, 134105/1−134105/11.
(26) Trani, F.; Scalmani, G.; Zheng, G. S.; Carnimeo, I.; Frisch, M. J.; Barone, V. *J. Chem. Theory Comput.* **2011**, *7*, 3304−3313.
(27) Cossi, M.; Rega, N.; Scalmani, G.; Barone, V. *J. Comput. Chem.* **2003**, *24*, 669−681.
(28) Bader, R. F. W. *In Atoms in Molecules: A Quantum Theory*; Oxford University Press: Oxford, U.K., 1990.
(29) Keith, T. A. *AIMAll*, version 12.06.03; TK Gristmill Software: Overland Park, KS, 2003. aim.tkgristmill.com.

DOI: 10.1021/acs.inorgchem.5b02506
Inorg. Chem. XXXX, XXX, XXX−XXX